

Neuronal Excitability

Glutamate Transporters EAAT2 and EAAT5 Differentially Shape Synaptic Transmission from Rod Bipolar Cell Terminals

Fu-Sheng Tang,* He-Lan Yuan,* Jun-Bin Liu, Gong Zhang, Si-Yun Chen, and  Jiang-Bin Ke<https://doi.org/10.1523/ENEURO.0074-22.2022>

State Key Laboratory of Ophthalmology, Zhongshan Ophthalmic Center, Sun Yat-sen University, Guangdong Provincial Key Laboratory of Ophthalmology and Visual Science, Guangzhou 510060, China

Abstract

Excitatory amino acid transporters (EAATs) control visual signal transmission in the retina by rapidly removing glutamate released from photoreceptors and bipolar cells (BCs). Although it has been reported that EAAT2 and EAAT5 are expressed at presynaptic terminals of photoreceptors and some BCs in mammals, the distinct functions of these two glutamate transporters in retinal synaptic transmission, especially at a single synapse, remain elusive. In this study, we found that EAAT2 was expressed in all BC types while coexisting with EAAT5 in rod bipolar (RB) cells and several types of cone BCs from mice of either sex. Our immunohistochemical study, together with a recently published literature (Gehlen et al., 2021), showed that EAAT2 and EAAT5 were both located in RB axon terminals near release sites. Optogenetic, electrophysiological and pharmacological analyses, however, demonstrated that EAAT2 and EAAT5 regulated neurotransmission at RB→All amacrine cell synapses in significantly different ways: EAAT5 dramatically affected both the peak amplitude and kinetics of postsynaptic responses in Alls, whereas EAAT2 had either relatively small or opposite effects. By contrast, blockade of EAAT1/GLAST, which was exclusively expressed in Müller cells, showed no obvious effect on All responses, indicating that glutamate uptake by Müller cells did not influence synaptic transmission from RB terminals. Furthermore, we found that temporal resolution at RB→All synapses was reduced substantially by blockade of EAAT5 but not EAAT2. Taken together, our work reveals the distinct functions of EAAT2 and EAAT5 in signal transmission at RB ribbon synapses.

Key words: amacrine cell; bipolar cell; glutamate transporter; retina; synaptic transmission; temporal resolution

Significance Statement

Excitatory amino acid transporters (EAATs) ensure normal information transfer between neurons by rapidly removing glutamate from the synaptic cleft. Although it has been reported that EAAT2 and EAAT5 are expressed at presynaptic terminals of photoreceptors and some bipolar cells (BCs) in the mammalian retina, their functional roles in visual signal transmission remain elusive. Here, we report that EAAT2 and EAAT5 coexist in rod bipolar (RB) cell terminals near release sites, but they influence glutamatergic transmission at RB→All amacrine cell synapses in significantly different ways, likely via distinct mechanisms. Furthermore, EAAT5 but not EAAT2 plays a predominant role in regulating temporal resolution at RB→All synapses. Our work therefore reveals the distinct functions of EAAT2 and EAAT5 in signal transmission from RB terminals.

Received February 16, 2022; accepted May 2, 2022; First published May 6, 2022.

The authors declare no competing financial interests.

Author contributions: J.-B.K. designed research; F.-S.T., H.-L.Y., J.-B.L., G.Z., and S.-Y.C. performed research; F.-S.T., H.-L.Y., J.-B.L., and J.-B.K. analyzed data; F.-S.T. and J.-B.K. wrote the paper.

Introduction

Glutamate, the major excitatory neurotransmitter in the retina, is released primarily by photoreceptors and bipolar cells (BCs), the first-order and second-order retinal neurons, respectively, in the canonical vertical pathway (Masland, 2012; Euler et al., 2014). Both photoreceptors and BCs transmit visual information to postsynaptic neurons through ribbon synapses, named for the existence of a specialized organelle, the synaptic ribbon, which holds synaptic vesicles close to release sites in presynaptic active zones (Matthews and Fuchs, 2010; Cho and von Gersdorff, 2012; Lagnado and Schmitz, 2015). Graded membrane potential changes induce fast and continuous vesicle exocytosis at these ribbon synapses, which will in turn lead to high concentrations of glutamate within the synaptic cleft (Matthews and Fuchs, 2010; Cho and von Gersdorff, 2012; Lagnado and Schmitz, 2015). Excitatory amino acid transporters (EAATs), then, are essential for rapid removal of glutamate from the synaptic cleft to ensure normal synaptic transmission and prevent excitotoxicity (Seal and Amara, 1999; Tzingounis and Wadiche, 2007; Rodríguez-Campuzano and Ortega, 2021).

To date, five subtypes of EAATs, namely, EAAT1–EAAT5, have been identified (Kanai and Hediger, 1992; Pines et al., 1992; Storck et al., 1992; Fairman et al., 1995; Arriza et al., 1997). Previous studies have shown different expression patterns of EAATs in the mammalian retina mainly by immunohistochemistry. In this study, we focused on EAAT2 and EAAT5, both of which served as presynaptic glutamate transporters in retinal neurons as reported previously. EAAT2 (also called GLT-1) is expressed in rod and cone photoreceptors as well as in certain types of BCs in the retinas of various species (Rauen and Kanner, 1994; Rauen et al., 1996, 2004; Eliasof et al., 1998a,b; Harada et al., 1998; Haverkamp and Wässle, 2000; Reye et al., 2002a,b; Fyk-Kolodziej et al., 2004). Interestingly, EAAT5 also has been reported to be expressed in photoreceptors and some BCs, including rod bipolar (RB) cells, in the mouse and rat retinas (Pow and Barnett, 2000; Wersinger et al., 2006). Therefore, EAAT2 and EAAT5 are likely to be co-expressed in photoreceptors. Whether EAAT2 and EAAT5 may coexist in any certain type of BCs is unknown, but an immunohistochemical study in the rat retina has shown that GLT-1B, a splice variant of EAAT2, is expressed in some, but not all, RBs (Reye et al., 2002a), suggesting the coexistence of EAAT2 and EAAT5 in rat retinal RBs.

This work was supported by the Fundamental Research Funds of State Key Laboratory of Ophthalmology, Sun Yat-sen University (J.-B.K.).

Acknowledgement: We thank Ting-Ting Zhang and Min Gao for technical assistance.

*F.-S.T. and H.-L.Y. contributed equally to this work.

Correspondence should be addressed to Jiang-Bin Ke at kejianbin@mail.sysu.edu.cn or jbke99@hotmail.com.

<https://doi.org/10.1523/ENEURO.0074-22.2022>

Copyright © 2022 Tang et al.

This is an open-access article distributed under the terms of the Creative Commons Attribution 4.0 International license, which permits unrestricted use, distribution and reproduction in any medium provided that the original work is properly attributed.

The distinct roles that EAAT2 and EAAT5 may play in synaptic transmission in the retina, however, remain elusive. While EAAT2 in salamander, goldfish or zebrafish cone photoreceptors has been reported to modify the responses in postsynaptic horizontal cells or BCs (Vandenbranden et al., 1996; Gaal et al., 1998; Niklaus et al., 2017), blockade of EAAT2 does not influence neurotransmission at mouse rod→RB synapses (Hasegawa et al., 2006). Instead, at the same synapses, EAAT5 has been demonstrated to play a predominant role, most likely by rapidly removing glutamate from the synaptic cleft (Hasegawa et al., 2006). EAAT5 located at RB axon terminals, however, is generally thought to function as glutamate-activated anion conductance and provide feedback inhibition to control RB output (Veruki et al., 2006; Wersinger et al., 2006; Ichinose and Lukasiewicz, 2012; Vandenberg and Ryan, 2013; Machtens et al., 2015; Fahlke et al., 2016; Bligard et al., 2020; Lukasiewicz et al., 2021; Kovermann et al., 2022). Additionally, a more recent study with EAAT5 knock-out mice reveals an important role of EAAT5 for improving temporal resolution in the retina, primarily by affecting signal transmission in the rod bipolar pathway (Gehlen et al., 2021). Given that both rods and RBs, the essential neurons in the rod bipolar pathway, express EAAT5, the exact sites that may influence temporal resolution remain to be determined.

In the present work, by conducting single-cell (sc)RNA sequencing (scRNA-seq) and scRT-PCR analyses, we found that EAAT2 was expressed in all mouse retinal BCs and coexisted with EAAT5 in RBs and some cone BC types. Immunohistochemical study further showed that EAAT2 was expressed in RB axon terminals at sites near ribbons. Optogenetic studies of neurotransmission at RB→All amacrine cell synapses combined with pharmacological analysis revealed that EAAT2 and EAAT5 differentially shaped signal transmission from RB terminals. Furthermore, we demonstrated that blockade of presynaptic EAAT5 but not EAAT2 compromised temporal resolution at RB→All synapses.

Materials and Methods

Animals

All animal procedures were performed in accordance with Sun Yat-sen University animal care committee's regulations. The transgenic mice, in which channelrhodopsin-2 (ChR2) was expressed predominantly in RBs, were obtained by crossing BAC-Pcp2-IRES-Cre mice (B6.Cg-Tg(Pcp2-cre)^{3555Jdh/J}; Jax 010536) with Ai32 mice (B6.Cg-Gt(ROSA)26Sor^{tm32(CAG-COP4*H134R/EYFP)Hze/J}; Jax 012569; Zhang et al., 2005; Ivanova et al., 2010; Madisen et al., 2012). The wild-type C57BL/6J and ChR2 mice of either sex at the ages between 6 and 12 weeks were used in electrophysiological experiments, and wild-type mice of either sex at the ages of postnatal day (P)17 and P42–P84 were used for scRT-PCR and immunohistochemical studies.

Electrophysiology

Retinal slices were cut at a thickness of 200 μm from light-adapted retinas isolated from both ChR2 and wild-

Table 1: Primers for scRT-PCR analysis

Gene	Protein	Forward primer (5'–3')	Reverse primer (5'–3')
<i>Slc1a2</i>	EAAT2	CTGATGTGGTCATGTTGATAGCC	AACTGGAGATGATAAGAGGGAGG
<i>Slc1a7</i>	EAAT5	TGGCATACTACCTGTGGACTAC	CTTGGTGC GG TACTGTTTGAA
<i>Prkca</i>	PKC α	GTTTACCCGGCCAACGACT	GGGCGATGAATTTGTGGTCTT

EAAT2, excitatory amino acid transporter 2; EAAT5, excitatory amino acid transporter 5; PKC α , protein kinase C α .

type mice. Retinas were dissected from enucleated eyes in oxygenated (95% O₂ and 5% CO₂) Ames' medium (Sigma), and then embedded in low-melting temperature agarose (Sigma type VIIA, 2–3% in a HEPES buffered saline). Slices were cut on a Leica VT1200s vibratome and stored in oxygenated Ames' medium at room temperature until use.

Recordings were performed at near-physiological temperature (30–34°C). Slices were perfused continuously (1–2 ml/min) with oxygenated artificial CSF (ACSF) containing (in mM): 119 NaCl, 23 NaHCO₃, 1.25 NaH₂PO₄, 2.5 KCl, 1.15 CaCl₂, 1.5 MgCl₂, 10 glucose, 2 Na-Lactate, and 2 Na-Pyruvate. 2-Amino-4-phosphonobutyrate (L-AP4; 5 μ M) and (S)-1-(2-amino-2-carboxyethyl)-3-(2-carboxy-5-phenylthiophene-3-yl-methyl)-5-methylpyrimidine-2,4-dione (ACET; 1 μ M) were included in the ACSF to block all synaptic transmission between photoreceptors and BCs. Picrotoxin (50 μ M),

4-imidazoleacetic acid (I4AA; 10 μ M) or (1,2,5,6-tetrahydropyridin-4-yl) methylphosphinic acid (TPMPA; 50 μ M), and strychnine (0.5 μ M) were added to the ACSF to block both GABA and glycine receptors. For All's voltage-clamp recordings, ACSF was also supplemented with tetrodotoxin (TTX; 0.5 μ M) to block voltage-gated sodium channels.

For voltage-clamp recordings, pipette solution contained (in mM): 95 Cs-methanesulfonate, 20 TEA-Cl, 1 4-AP, 10 HEPES, 8 PO₄-creatine, 4 ATP-Mg, 0.4 GTP-Na₃, and 1 BAPTA. For current-clamp recordings, pipette solution contained (in mM): 110 K-gluconate, 5 NaCl, 10 HEPES, 8 PO₄-creatine, 4 ATP-Mg, 0.4 GTP-Na₃, and 1 BAPTA. The pH was adjusted to 7.2 with CsOH (for Cs-based pipette solution) or KOH (for K-based pipette solution), and osmolarity to ~285 mOsm with sucrose. In some cases, Alexa Fluor 594 or Alexa Fluor 488 was

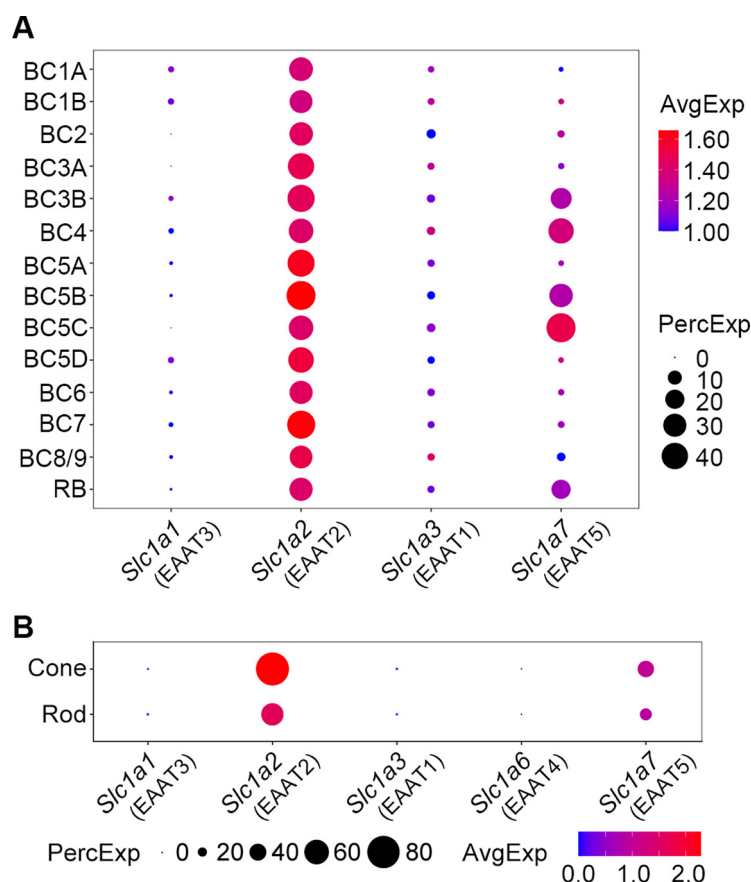


Figure 1. scRNA-seq data analysis reveals gene expression of EAAT2 in all mouse retinal BCs and co-expression with EAAT5 in several BC types. **A**, Gene expression patterns of EAATs in different types of BCs. The protein that each gene encodes is given in parentheses. The size of each circle represents the percentage of cells in the group (PercExp) in which the gene expression is detected. The color represents the average transcript count in expressing cells (AvgExp). BC, bipolar cell; RB, rod bipolar cell. **B**, Co-expression of EAAT2 and EAAT5 in cone and rod photoreceptors.

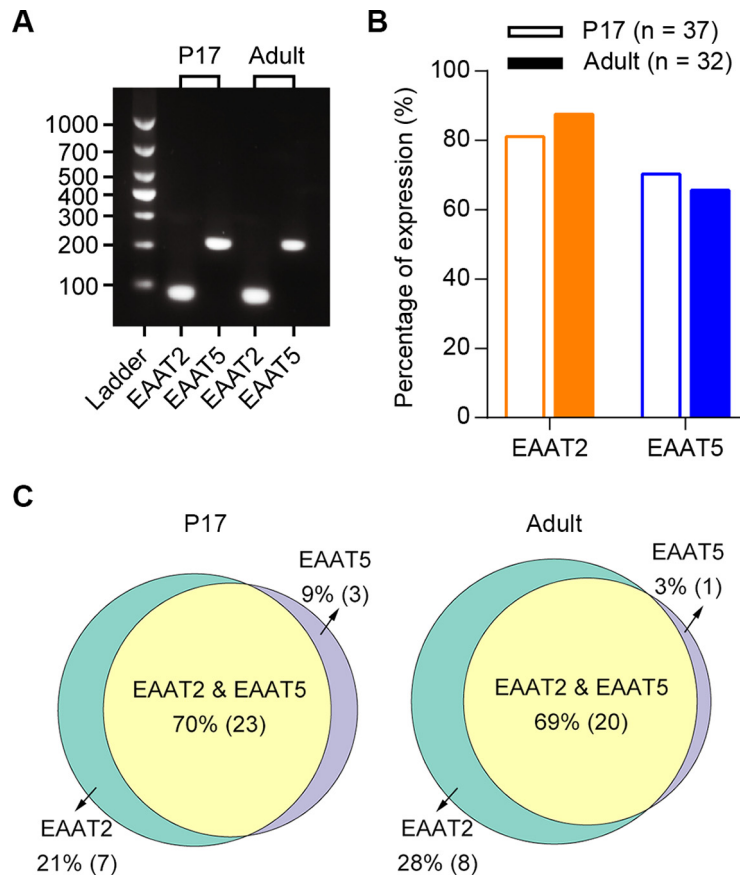


Figure 2. Co-expression of EAAT2 and EAAT5 in mouse retinal RBs is confirmed by scRT-PCR analysis. **A**, scRT-PCR analyses of EAAT2 and EAAT5 mRNA expression in a single RB cell from a P17 mouse retina and the other RB from an adult mouse retina. Co-expression of EAAT2 and EAAT5 could be seen in both RBs. A ladder with DNA fragments between 100 and 1000 bp is shown on the left. **B**, The percentages of EAAT2 and EAAT5 expression in individual RBs from both P17 and adult mice. See also Table 2. **C**, Schematic diagrams illustrating the molecular heterogeneity for EAAT2 and EAAT5 expression in individual RBs from P17 and adult mice. The percentages of either subtype and a combination of EAAT2 and EAAT5 are shown, and the exact cell numbers are given in parentheses. See also Table 3.

included in the pipettes and epifluorescence images were taken to confirm the cell types. Generally, All was held at -80 mV, and membrane potentials were corrected for junction potentials of ~ -10 mV. Access resistances were <30 M Ω for RBs and <20 M Ω for Alls and were compensated by 50–90%. Electrical signals were recorded using MultiClamp 700B amplifiers, sampled at 10–20 kHz and low-pass filtered at 2 kHz by an ITC-18 A/D board (Heka/Instrutech) controlled by software written in Igor Pro 6 (WaveMetrics). Recordings were analyzed in Igor Pro 6.

Dihydrokainic acid (DHK) was obtained from Santa Cruz Biotechnology and Tocris, GT949 was from Absin, UCPH101 was from Abcam, and other chemicals were from Tocris or Sigma-Aldrich. Agents were dissolved in dimethylsulfoxide (DMSO) where appropriate and then diluted into the superfusion solution [with final concentrations of DMSO $<0.1\%$ (v/v) in all experiments].

Optogenetics

ChR2 was activated by a 470-nm high-power LED (Thor Laboratories) directed through a $60\times$ lens to generate a light spot with ~ 125 - μ m diameter. The stimulus paradigm

(e.g., light intensities and durations) was controlled by the data acquisition software (Igor Pro 6).

Fraction of correct responses

To assess the effects of drugs on temporal resolution at RB→All synapses, light stimulus with a train of 10

Table 2: Expression of EAAT2 and EAAT5 in P17 and adult mouse retinal RBs

	EAAT2	EAAT5
P17 mice		
Total RB number	37	37
Positive RB number	30	26
Negative RB number	7	11
Percentage of expression	81.08%	70.27%
Adult mice		
Total RB number	32	32
Positive RB number	28	21
Negative RB number	4	11
Percentage of expression	87.50%	65.63%

EAAT2, excitatory amino acid transporter 2; EAAT5, excitatory amino acid transporter 5; P17, postnatal day 17; RB, rod bipolar cell.

Table 3: Molecular heterogeneity of EAAT2 and EAAT5 in individual mouse retinal RBs

	P17 mice		Adult mice	
	RB number	Percentage	RB number	Percentage
EAAT2 alone	7	21.21%	8	27.59%
EAAT5 alone	3	9.09%	1	3.45%
EAAT2 and EAAT5	23	69.70%	20	68.97%
Total	33		29	

EAAT2, excitatory amino acid transporter 2; EAAT5, excitatory amino acid transporter 5; P17, postnatal day 17; RB, rod bipolar cell.

consecutive flashes was used to activate ChR2-expressing RBs at various frequencies between 2 and 50 Hz, and the responses in AIs were recorded and analyzed. The AI response to an individual flash was considered correct when a significant membrane potential change (depolarization in this case) was visible, and the fraction of correct responses (with a value between 0 and 1) was determined as the proportion of correct responses to a stimulus train of 10 flashes.

Analysis of scRNA-seq datasets

The existing scRNA-seq dataset (GEO accession number: GSE81905) that contains transcriptomes of all mouse retinal BCs (Shekhar et al., 2016) was re-analyzed to determine EAAT subtypes in BCs specifically. To

reproduce clustering analysis, the clustering algorithm for the retinal BC data achieved with Vsx2-GFP mice at P17 was implemented and performed using a published R markdown script (Shekhar et al., 2016). The single-cell libraries that contained >10% mitochondrially-derived transcripts were filtered. Batch correction and principal component analysis (PCA) were performed on the cells for which over 500 genes were detected. Among the selected cells, only genes that were present in at least 30 cells and those having over 60 transcripts were considered. Based on the Louvain–Jaccard method (Blondel et al., 2008; Levine et al., 2015), PC scores were used to embed the single cells on a 2D map using t-distributed stochastic neighbor embedding (t-SNE; van der Maaten and Hinton, 2008). The gene expression patterns of EAAT subtypes across BC clusters were shown in

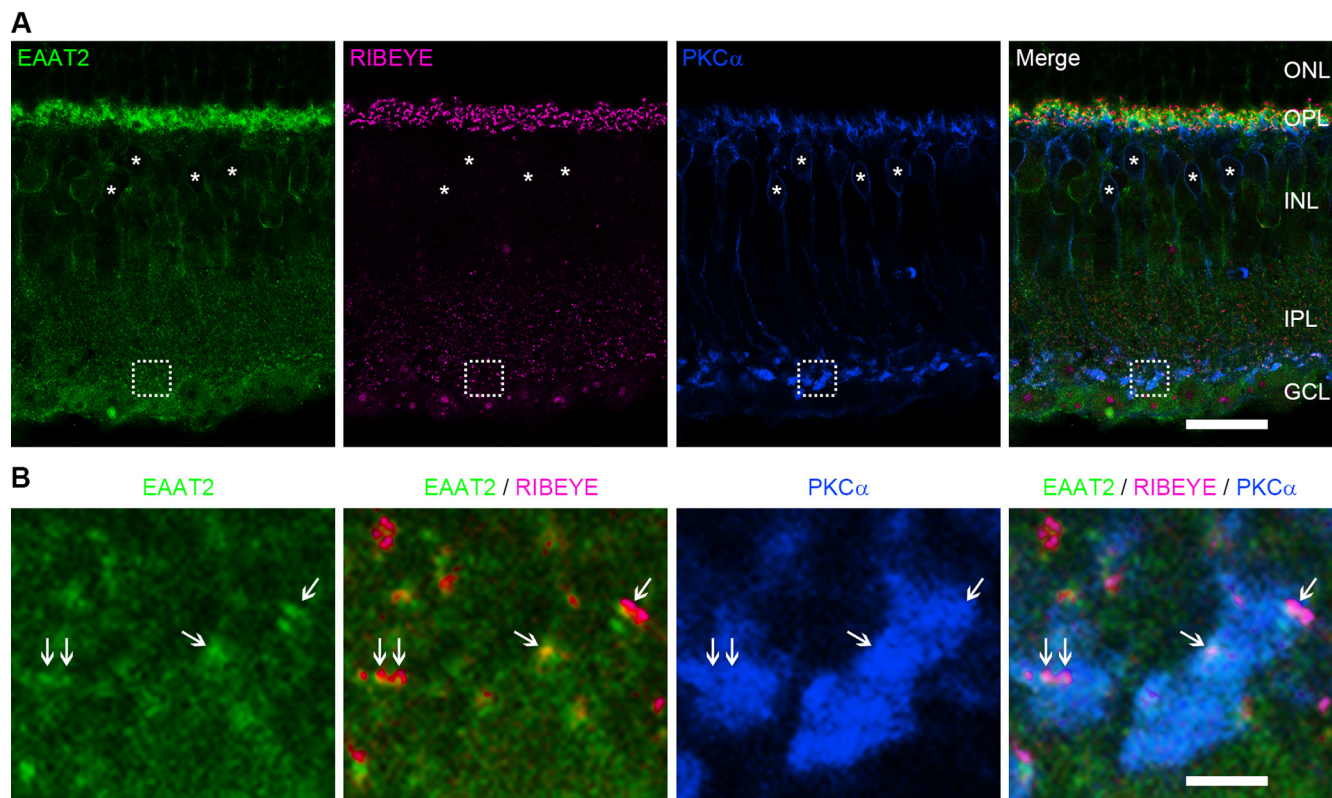


Figure 3. EAAT2 is located near ribbons in the axon terminals of RBs. **A**, Confocal images showing immunofluorescence triple labeling of EAAT2 (green), RIBEYE (magenta), and PKC α (blue) in a frozen mouse retinal section. EAAT2 was expressed strongly in the OPL, and moderately in the INL, IPL, and GCL. Note that, in the INL, EAAT2 was expressed in the somata of some cone bipolar cells but not RB cells labeled by PKC α (asterisks). ONL, outer nuclear layer; OPL, outer plexiform layer; INL, inner nuclear layer; IPL, inner plexiform layer; GCL, ganglion cell layer. Scale bar: 20 μ m. **B**, Magnification of the images in the dashed line frames of **A**. EAAT2 was expressed in RB axon terminals at sites near ribbons (arrows). Scale bar: 2.5 μ m.

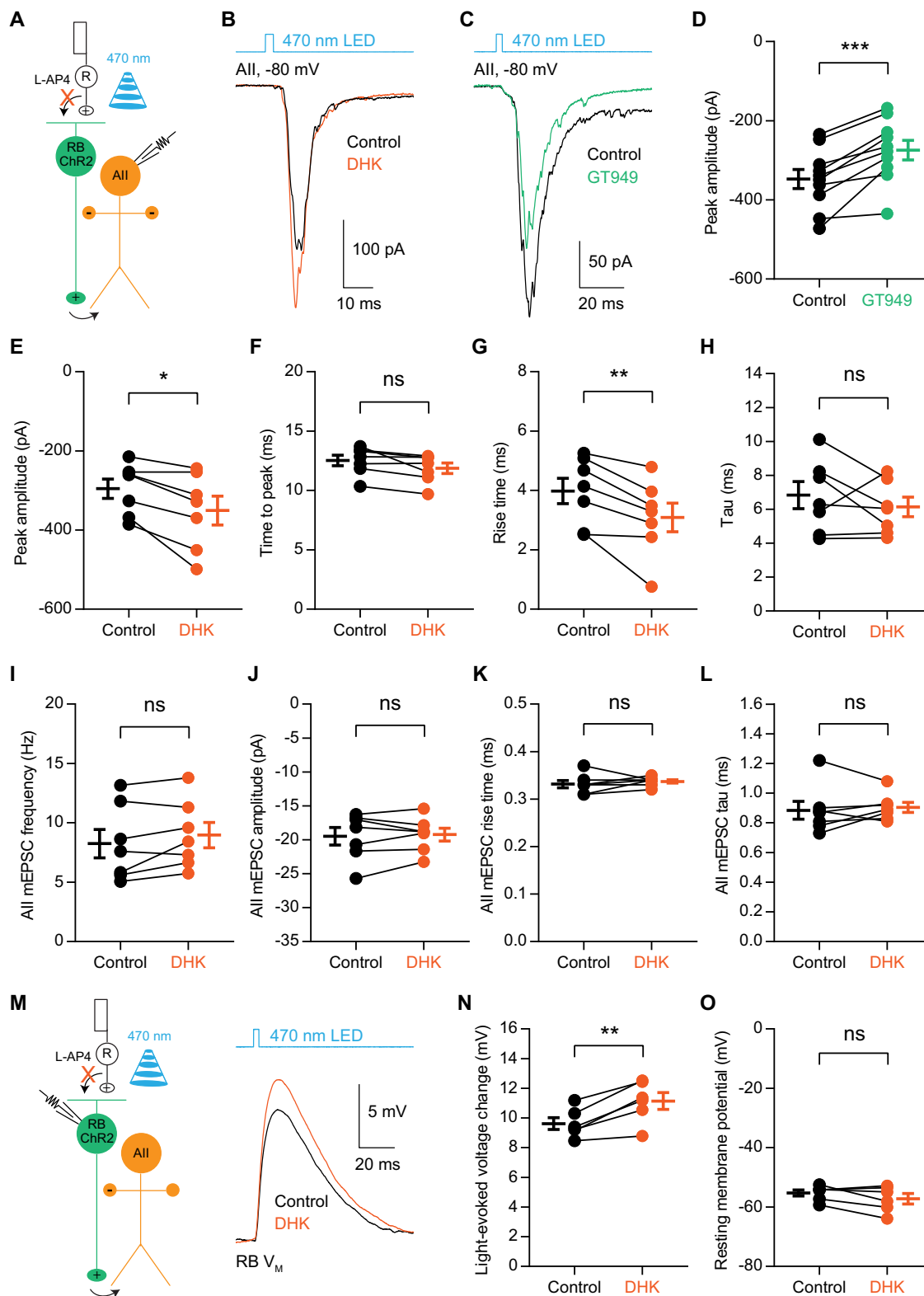


Figure 4. EAAT2 regulates signal transmission at RB→All ribbon synapses. **A**, A schematic diagram showing the optogenetic study of neurotransmission between RBs and All amacrine cells. ChR2 was expressed predominantly in RBs by cre-dependent recombination in adult *Pcp2-cre::Ai32* mouse retinas. With all the synaptic transmission between photoreceptors and BCs is blocked pharmacologically, brief flashes of 470-nm LED light can directly activate ChR2+ RBs and induce postsynaptic responses in Alls, which mainly reflect neurotransmitter release from RBs. The electrical coupling between ChR2+ ON cone bipolar cells and Alls is negligible under this experimental condition (Liang et al., 2021). R, rod. **B**, The EPSCs recorded in Alls, which were evoked by 470-nm LED light stimulation, were enhanced by 200 μ M DHK, a selective EAAT2 blocker. $V_{\text{hold}} = -80$ mV. **C**, The ChR2-evoked EPSCs

continued

were reduced by 10 μM GT949, a positive allosteric modulator of EAAT2. **D, E**, Summary data showing the effects of GT949 ($n = 10$) and DHK ($n = 7$) on the peak amplitude of All EPSCs. **F**, DHK reduced the time to peak of EPSCs slightly, but not significantly ($n = 7$, $p = 0.0531$). **G**, DHK reduced the rise time of EPSCs ($n = 7$). **H**, DHK did not change the decay time (τ) of EPSCs ($n = 7$). **I–L**, DHK did not affect the frequency, amplitude, rise time, or τ of mEPSCs recorded in Alls ($n = 7$). mEPSCs, miniature EPSCs. **M**, The voltage changes in ChR2+ RBs, which were evoked by brief flashes of 470-nm LED light, were increased by 200 μM DHK. **N**, DHK increased the voltage changes in RBs evoked by light flashes ($n = 6$). **O**, DHK did not influence the resting membrane potentials of RBs ($n = 6$). The data were represented as mean \pm SEM. Wilcoxon signed-rank test or Student's t test was used where appropriate. * $p < 0.05$, ** $p < 0.01$; ns, not significantly different. See also Table 4.

dotplots, which illustrated the proportion of different BC clusters (row) that expressed EAAT subtypes (column) using dot size and the average number of EAAT subtype transcripts in specific BC cluster using dot color.

Another existing dataset (GEO accession number: GSE63473), which contained the information about transcriptomes of individual cone and rod photoreceptors from the mouse retinas, was used to examine the transcripts of EAAT subtypes in photoreceptors (Macosko et al., 2015).

scRT-PCR analysis

The cytoplasmic contents of individual RBs on freshly cut retinal slices were harvested using patch pipettes. Patch pipettes (6–8 M Ω) were pulled from capillaries previously autoclaved and filled with the pipette solution used for current-clamp recordings (above). To better preserve mRNAs, Recombinant Ribonuclease Inhibitor (RRI; 2.5%; catalog #2313A, Clontech) was included in the pipette solution. After establishing whole-cell configuration, the cytoplasm was harvested into the pipette by applying slight negative pressure. The pipette solution without any harvested cell content was used as a negative control.

The harvested cell contents were processed for reverse transcription and sequence-specific amplification using the Single Cell Sequence Specific Amplification kit (catalog #P621-A, Vazyme Biotech). Specific primer pairs (Table 1) were pooled to prepare an Assay Pool (with a final concentration of 0.1 μM for each pair). Then the content of the patch pipette was transferred into PCR tubes with Reaction Mix, Assay Pool, and RT/Taq enzyme. PCR tubes were instantly frozen at -80°C . The tubes were placed on PCR machine following brief centrifugation at 25°C . Thermal cycling conditions were 50°C for 1 h (reverse transcription), 3 min at 95°C (reverse transcriptase inactivation and Taq polymerase activation), followed by preamplification with 20 cycles of 15 s at 95°C (denaturation), 15 min at 60°C (annealing/extension). Subsequently, preamplification products were diluted to 50-fold and reamplified by another round of PCR with specific primer pairs (with a final concentration of 10 μM for each pair) for targeted genes (Table 1) using Phanta Max Super-Fidelity DNA Polymerase (catalog #P505-d1/d2/d3, Vazyme Biotech). PCR experiments were performed following manufacturer's instructions with an appropriate annealing temperature (56°C) for 35 cycles. RT-PCR products (10 μl for each one) were electrophoresed through 3% agarose gel, stained with SYBR Safe DNA gel stain (catalog #S33102, Invitrogen) and

imaged under UV light excitation. RB identity was confirmed by detection of the *Prkca* gene during scRT-PCR analysis.

Immunohistochemistry

Retinas from both P17 and adult wild-type mice were harvested and fixed for 20 min in 4% PFA. Then retinas were incubated in graded (10%, 20%, and 30%) sucrose in PBS, embedded in OCT, and sectioned vertically with a cryostat (Leica). Thereafter, retinal sections (14- μm thickness) were treated with blocking solution [6% bovine serum albumin (BSA) in 0.1% Triton X-100 in PBS (PBST)] for 2 h at room temperature. After removal of the blocking solution, sections were incubated overnight at 4°C with primary antibodies as follows: rabbit anti-EAAT2 (1:100, catalog #250203, Synaptic Systems; the specificity of this antibody has been verified by EAAT2 knock-out mice as described by the manufacturer), mouse anti-PKC α (1:200, catalog #P5704, Sigma) and guinea pig anti-RIBEYE/CtBP2 (1:1000, catalog #192104, Synaptic Systems). The anti-EAAT2 antibody generated using the peptide immunogen (peptide sequence: LISSLITGLSGLDAK) can recognize all mouse EAAT2 splice variants. After rinsing, the sections were incubated in corresponding secondary antibodies including Alexa Fluor 568 donkey anti-rabbit (1:200, catalog #A10042, Thermo Fisher Scientific), Alexa Fluor 647 donkey anti-mouse (1:200, catalog #A31571, Thermo Fisher Scientific) and Alexa Fluor 488 goat anti-guinea pig (1:200, catalog #A11073, Thermo Fisher Scientific) for 2 h in darkness at room temperature. All antibodies were diluted in PBST with 3% BSA. Control experiments were conducted either by omission of primary antibodies or by preincubation of primary antibodies with the corresponding immunopeptides. A Zeiss LSM 880 laser-scanning confocal microscope with a Plan-Apochromat 63 \times /1.4 oil-immersion objective was used for immunofluorescence imaging. Images were edited using Photoshop software (Adobe Systems) and ZEN software (Carl Zeiss).

Statistical analysis

Prism 8 (GraphPad software) was used to perform the statistical analysis. Original data were used for all the pairwise comparisons; and, for comparisons between different groups, data acquired from each cell were normalized to the value under control condition. Differences between experimental samples were assessed using Student's t test, Welch's t test or Wilcoxon signed-rank test, depending on whether the data passed the normality criterion (Kolmogorov–Smirnov test) or not. Significance was accepted as $p < 0.05$. All data were presented as mean \pm SEM.

Table 4: The effects of EAAT2-related drugs on All responses and RB membrane potentials

	Data	Data structure	Type of test	Power	Mean \pm SEM	Number of cells
	Effect of DHK on All EPSC amplitude (unit: pA)					
	Control	Normal distribution			-295.40 ± 24.45	7
	200 μM DHK	Normal distribution			-350.70 ± 36.26	7
a	Control vs DHK		Paired Student's <i>t</i> test	$p = 0.0111$		7
	Effect of GT949 on All EPSC amplitude (unit: pA)					
	Control	Normal distribution			-347.50 ± 24.07	10
	10 μM GT949	Normal distribution			-274.40 ± 24.73	10
b	Control vs GT949		Paired Student's <i>t</i> test	$p = 0.0004$		10
	Relative effects of DHK and GT949 on All EPSC amplitude					
	Control	Non-normal distribution			1.00 ± 0.00	
	200 μM DHK	Normal distribution			1.18 ± 0.04	7
	10 μM GT949	Normal distribution			0.78 ± 0.03	10
c	Control vs DHK		Wilcoxon signed-rank test	$p = 0.0313$		7
d	Control vs GT949		Wilcoxon signed-rank test	$p = 0.0020$		10
	Effect of DHK on All EPSC time to peak (unit: ms)					
	Control	Normal distribution			12.53 ± 0.44	7
	200 μM DHK	Normal distribution			11.87 ± 0.44	7
e	Control vs DHK		Paired Student's <i>t</i> test	$p = 0.0531$		7
	Effect of DHK on All EPSC rise time (unit: ms)					
	Control	Normal distribution			3.98 ± 0.43	7
	200 μM DHK	Normal distribution			3.09 ± 0.48	7
f	Control vs DHK		Paired Student's <i>t</i> test	$p = 0.0050$		7
	Effect of DHK on All EPSC tau (unit: ms)					
	Control	Normal distribution			6.73 ± 0.80	7
	200 μM DHK	Normal distribution			6.03 ± 0.58	7
g	Control vs DHK		Paired Student's <i>t</i> test	$p = 0.3519$		7
	Effect of DHK on All mEPSC frequency (unit: Hz)					
	Control	Normal distribution			8.25 ± 1.20	7
	200 μM DHK	Normal distribution			8.97 ± 1.07	7
h	Control vs DHK		Paired Student's <i>t</i> test	$p = 0.1120$		7
	Effect of DHK on All mEPSC amplitude (unit: pA)					
	Control	Normal distribution			-19.47 ± 1.30	7
	200 μM DHK	Normal distribution			-19.23 ± 0.95	7
i	Control vs DHK		Paired Student's <i>t</i> test	$p = 0.6892$		7
	Effect of DHK on All mEPSC rise time (unit: ms)					
	Control	Normal distribution			0.33 ± 0.01	7
	200 μM DHK	Non-normal distribution			0.34 ± 0.00	7
j	Control vs DHK		Wilcoxon signed-rank test	$p = 0.3750$		7
	Effect of DHK on All mEPSC tau (unit: ms)					
	Control	Non-normal distribution			0.88 ± 0.06	7
	200 μM DHK	Normal distribution			0.90 ± 0.03	7
k	Control vs DHK		Wilcoxon signed-rank test	$p = 0.5781$		7
	Effect of DHK on RB light-evoked voltage change (unit: mV)					
	Control	Normal distribution			9.62 ± 0.39	6
	200 μM DHK	Normal distribution			11.14 ± 0.56	6
l	Control vs DHK		Paired Student's <i>t</i> test	$p = 0.0036$		6
	Effect of DHK on RB resting membrane potential (unit: mV)					
	Control	Normal distribution			-55.28 ± 1.04	6
	200 μM DHK	Normal distribution			-57.21 ± 1.76	6
m	Control vs DHK		Paired Student's <i>t</i> test	$p = 0.1574$		6

DHK, a selective EAAT2 blocker; GT949, a positive allosteric modulator of EAAT2; All, All amacrine cell; RB, rod bipolar cell.

Results

Analysis of scRNA-seq data reveals gene expression of EAAT2 in all mouse retinal BCs and co-expression with EAAT5 in several BC types

In a recent study, scRNA-seq has been used for molecular classification of mouse retinal BCs, and consequently, the transcriptomes of multiple molecularly defined BC types,

including the RB, are available in the Gene Expression Omnibus Database (GEO accession number: GSE81905; Shekhar et al., 2016). We began by re-analyzing this dataset with particular attention to the transcripts of EAAT-related genes. The dotplots in Figure 1 illustrate the average expression level (color) for each BC type and the percentage of EAAT expressing cells (circle size). Surprisingly, we found that EAAT2 transcripts were expressed at relatively high

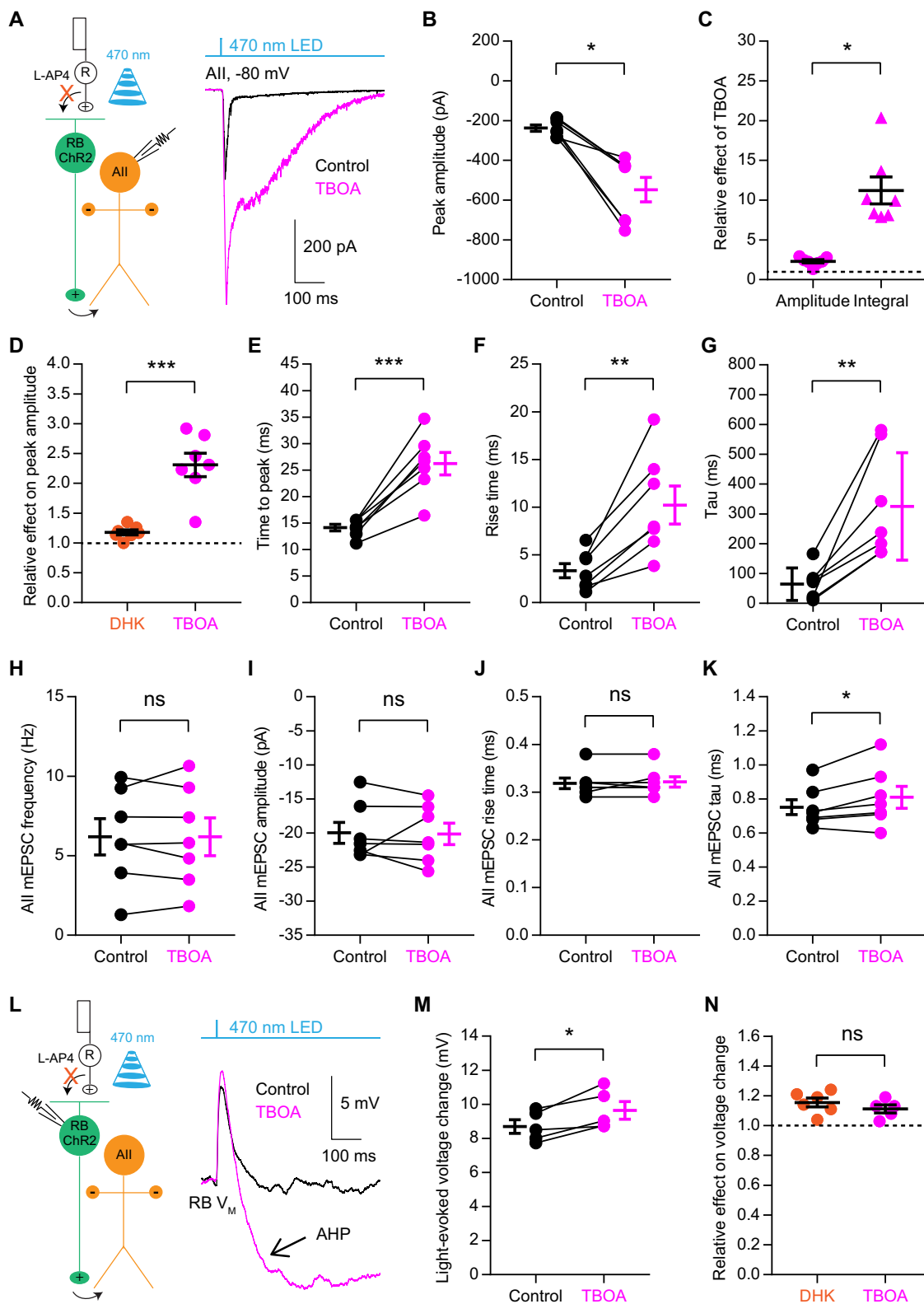


Figure 5. Pharmacological blockade of all EAATs has a significant effect on signal transmission at RB→All synapses. **A**, The EPSCs recorded in All amacrine cells, which were evoked by activating ChR2+ RBs with 470-nm LED light stimulation, were enhanced by 50 μ M TBOA, a nonselective blocker of all EAATs. $V_{\text{hold}} = -80$ mV. R, rod; RB, rod bipolar cell; Chr2, channelrhodopsin-2. **B**, TBOA increased the peak amplitude of ChR2-evoked EPSCs ($n = 7$). **C**, The relative effects of TBOA on the peak amplitude and current integral of All EPSCs ($n = 7$). The peak amplitudes/integrals were normalized to the peak amplitude/integral under control condition in each cell before averaging across cells. **D**, Comparison of the relative effects of DHK ($n = 7$), a selective EAAT2 blocker, and TBOA

continued

($n=7$) on the peak amplitude of All EPSCs. **E–G**, TBOA changed the time to peak, rise time and tau of EPSCs ($n=7$). **H–K**, TBOA did not influence the frequency, amplitude, or rise time of mEPSCs recorded in Alls while increasing the tau slightly ($n=7$). mEPSCs, miniature EPSCs. **L**, The voltage changes in ChR2⁺ RBs, which were evoked by brief flashes of 470-nm LED light, were increased by 50 μ M TBOA. Note that, in the presence of TBOA, a large, long-lasting AHP (arrow) could be recorded in each RB following the light-evoked depolarization. **M**, TBOA increased the initial voltage changes in RBs evoked by light flashes ($n=5$). **N**, Comparison of the relative effects of DHK ($n=6$) and TBOA ($n=5$) on light-evoked voltage changes in RBs. The data were represented as mean \pm SEM. Wilcoxon signed-rank test or Student's *t* test was used where appropriate. * $p < 0.05$, ** $p < 0.01$, *** $p < 0.001$; ns, not significantly different. See also [Table 5](#).

levels in all BC types, while EAAT5 transcripts were expressed at reasonable levels in several types of BCs, more specifically, in RB, BC3B, and BC4 (types 3B and 4 OFF cone BCs, respectively) as well as in BC5B and BC5C (types 5B and 5C ON cone BCs, respectively; [Fig. 1A](#)). These findings were quite remarkable, because (1) expression of EAAT2 is thought to be restricted to only some BC types and (2) although it is well accepted that EAAT2 and EAAT5 coexist in rod and cone photoreceptors, co-expression of EAAT2 and EAAT5 in any certain type of BCs rarely has been reported in previous studies. As a control for these unexpected findings, we re-analyzed another existing scRNA-seq dataset (GEO accession number: GSE63473), which includes the transcriptomes for mouse retinal rod and cone photoreceptors ([Macosko et al., 2015](#)). We found that rod and cone photoreceptors showed much higher levels of mRNAs encoding EAAT2 and EAAT5 than other EAAT-related transcripts ([Fig. 1B](#)), consistent with previous studies ([Haverkamp and Wässle, 2000](#); [Pow and Barnett, 2000](#); [Rauen et al., 2004](#); [Wersinger et al., 2006](#)).

We therefore determined that EAAT2 is expressed in all BC types while coexisting with EAAT5 in RBs as well as in types 3B, 4, 5B, and 5C cone BCs.

Co-expression of EAAT2 and EAAT5 in mouse retinal RBs is confirmed by scRT-PCR analysis

Next, we performed a targeted assessment of EAAT2 and EAAT5 transcripts in mouse RBs using scRT-PCR to confirm our observations from scRNA-seq analysis and to examine the potential heterogeneity of EAAT2 and EAAT5 expression in BCs. Since the existing scRNA-seq dataset (GEO accession number: GSE81905) was acquired from mouse retinas at P17 ([Shekhar et al., 2016](#)), we conducted scRT-PCR experiments using RBs from both P17 and adult (6- to 12-week-old) mice to determine whether there are developmental changes in EAAT2 and/or EAAT5 expression. Consistent with our scRNA-seq analysis, scRT-PCR detected both EAAT2 and EAAT5 mRNAs in individual RBs from P17 mice ($n=37$ cells) as well as from adult mice ($n=32$ cells; [Fig. 2A,B](#)). In general, the mRNA expression of EAAT2 and EAAT5 assessed by scRT-PCR was quite stable from P17 to adulthood ([Fig. 2B](#); [Table 2](#)).

It is noteworthy that although the expression profiles of EAAT2 and EAAT5 varied among individual cells within the population of RBs ([Fig. 2C](#); [Table 3](#)), most RBs expressed both EAAT2 and EAAT5: the specific combination of EAAT2 and EAAT5 was found in $\sim 70\%$ and 69% of EAAT2/EAAT5-expressing RBs from P17 and adult mice, respectively; this is in line with the scRNA-seq analysis ([Fig. 1A](#)).

In conclusion, it would seem that the majority of RBs co-express EAAT2 and EAAT5.

EAAT2 is located near ribbons in the axon terminals of RBs

Previous studies have shown in rat and mouse retinas that EAAT5 is located in RB axon terminals ([Pow and Barnett, 2000](#); [Wersinger et al., 2006](#)). In addition, a more recent study has reported that EAAT5 is expressed in a punctate manner near the release sites in the axon terminals of mouse RBs ([Gehlen et al., 2021](#)). To examine the subcellular localization and potential developmental changes of EAAT2 proteins, we performed fluorescent immunohistochemical labeling of EAAT2, PKC α (a specific cell marker of RBs), and RIBEYE (a ribbon-specific protein) in both P17 and adult mouse retinal sections. Consistent with the scRT-PCR results, no significant differences in the expression patterns of EAAT2 were observed between P17 and adult retinas. Hence, for simplicity, we present only the results from the adult retinas here.

EAAT2 was found to be expressed most prominently in the outer plexiform layer (OPL), moderately in the inner nuclear layer (INL) and throughout the inner plexiform layer (IPL) in a punctate manner ([Fig. 3A](#)). In the INL, immunolabeling for EAAT2 was observed on the cell membrane of some BCs which were not labeled by PKC α , indicating that EAAT2 is expressed in the somata of some cone BCs, but not RBs ([Fig. 3A](#)). Remarkably, we found that EAAT2 was located in the axon terminals of RBs at sites near ribbons ([Fig. 3B](#)), suggesting that EAAT2 might play an important role in regulating synaptic transmission from RB terminals.

EAAT2 regulates signal transmission at RB→All ribbon synapses

Our immunohistochemical study, together with a recently published literature ([Gehlen et al., 2021](#)), indicate that EAAT2 and EAAT5 are both located near the release sites in the axon terminals of mouse RBs. The distinct roles that EAAT2 and EAAT5 may play in signal transmission at RB→All synapses, however, remains elusive. It has been shown recently that, by expressing the light-sensitive cation channel ChR2 predominantly in RBs using cre-mediated recombination in the *Pcp2-cre::Ai32* mouse retina, optogenetic stimulation of neurotransmission at RB→All synapses could be stable over long periods (>20 min; [Liang et al., 2021](#)). To determine whether EAAT2 and EAAT5 contribute to synaptic transmission

Table 5: The effects of TBOA on All responses and RB membrane potentials

Data	Data structure	Type of test	Power	Mean \pm SEM	Number of cells
Effect of TBOA on All EPSC amplitude (unit: pA)					
Control	Normal distribution			-237.40 ± 16.21	7
50 μM TBOA	Non-normal distribution			-547.20 ± 61.50	7
a Control vs TBOA		Wilcoxon signed-rank test	$p = 0.0156$		7
Relative effects of TBOA on All EPSC amplitude and integral					
Control	Non-normal distribution			1.00 ± 0.00	7
50 μM TBOA (amplitude)	Normal distribution			2.31 ± 0.20	7
50 μM TBOA (integral)	Non-normal distribution			11.22 ± 1.70	7
b Control vs TBOA (amplitude)		Wilcoxon signed-rank test	$p = 0.0156$		7
c Control vs TBOA (integral)		Wilcoxon signed-rank test	$p = 0.0156$		7
d TBOA (amplitude) vs TBOA (integral)		Wilcoxon signed-rank test	$p = 0.0156$		7
Relative effect of DHK on All EPSC amplitude					
200 μM DHK	Normal distribution			1.18 ± 0.04	7
e DHK vs TBOA (amplitude)		Unpaired Student's <i>t</i> test	$p = 0.0001$		
Effect of TBOA on All EPSC time to peak (unit: ms)					
Control	Normal distribution			14.16 ± 0.62	7
50 μM TBOA	Normal distribution			26.21 ± 2.12	7
f Control vs TBOA		Paired Student's <i>t</i> test	$p = 0.0004$		7
Effect of TBOA on All EPSC rise time (unit: ms)					
Control	Normal distribution			3.34 ± 0.75	7
50 μM TBOA	Normal distribution			10.23 ± 1.99	7
g Control vs TBOA		Paired Student's <i>t</i> test	$p = 0.0032$		7
Effect of TBOA on All EPSC tau (unit: ms)					
Control	Non-normal distribution			64.54 ± 20.61	7
50 μM TBOA	Normal distribution			325 ± 68.02	7
h Control vs TBOA		Paired Student's <i>t</i> test	$p = 0.0050$		7
Effect of TBOA on All mEPSC frequency (unit: Hz)					
Control	Normal distribution			6.19 ± 1.14	7
50 μM TBOA	Normal distribution			6.19 ± 1.19	7
i Control vs TBOA		Paired Student's <i>t</i> test	$p = 0.9854$		7
Effect of TBOA on All mEPSC amplitude (unit: pA)					
Control	Normal distribution			-19.98 ± 1.55	7
50 μM TBOA	Normal distribution			-20.13 ± 1.57	7
j Control vs TBOA		Paired Student's <i>t</i> test	$p = 0.8856$		7
Effect of TBOA on All mEPSC rise time (unit: ms)					
Control	Non-normal distribution			0.32 ± 0.01	7
50 μM TBOA	Normal distribution			0.32 ± 0.01	7
k Control vs TBOA		Wilcoxon signed-rank test	$p > 0.9999$		7
Effect of TBOA on All mEPSC tau (unit: ms)					
Control	Normal distribution			0.75 ± 0.04	7
50 μM TBOA	Normal distribution			0.81 ± 0.06	7
l Control vs TBOA		Paired Student's <i>t</i> test	$p = 0.0392$		7
Effect of TBOA on RB light-evoked voltage change (unit: mV)					
Control	Normal distribution			8.69 ± 0.39	5
50 μM TBOA	Normal distribution			9.64 ± 0.51	5
m Control vs TBOA		Paired Student's <i>t</i> test	$p = 0.0192$		5
Effect of TBOA on RB resting membrane potential (unit: mV)					
Control	Normal distribution			-52.92 ± 2.01	5
50 μM TBOA	Normal distribution			-52.91 ± 2.95	5
n Control vs TBOA		Paired Student's <i>t</i> test	$p = 0.9931$		5
Relative effects of DHK and TBOA on RB light-evoked voltage change					
200 μM DHK	Normal distribution			1.16 ± 0.03	6
50 μM TBOA	Normal distribution			1.11 ± 0.03	5
o DHK vs TBOA		Unpaired Student's <i>t</i> test	$p = 0.3226$		

TBOA, a non-selective EAAT blocker; DHK, a selective EAAT2 blocker; All, All amacrine cell; RB, rod bipolar cell.

between RBs and AIs, we blocked all the transmission from photoreceptors to second-order retinal neurons (i.e., BCs and horizontal cells) with the mGluR6 agonist L-AP4 (5 μM) and the kainate receptor antagonist ACET (1 μM) and used brief flashes (2–10 ms) of 470-nm LED light to activate

RBs; optogenetically-evoked EPSCs and miniature EPSCs (mEPSCs) recorded in AIs under this condition reflect evoked and spontaneous release from RBs, respectively (Fig. 4A; Liang et al., 2021). As a control, no visible light-evoked EPSCs could be detected in AIs from wild-type

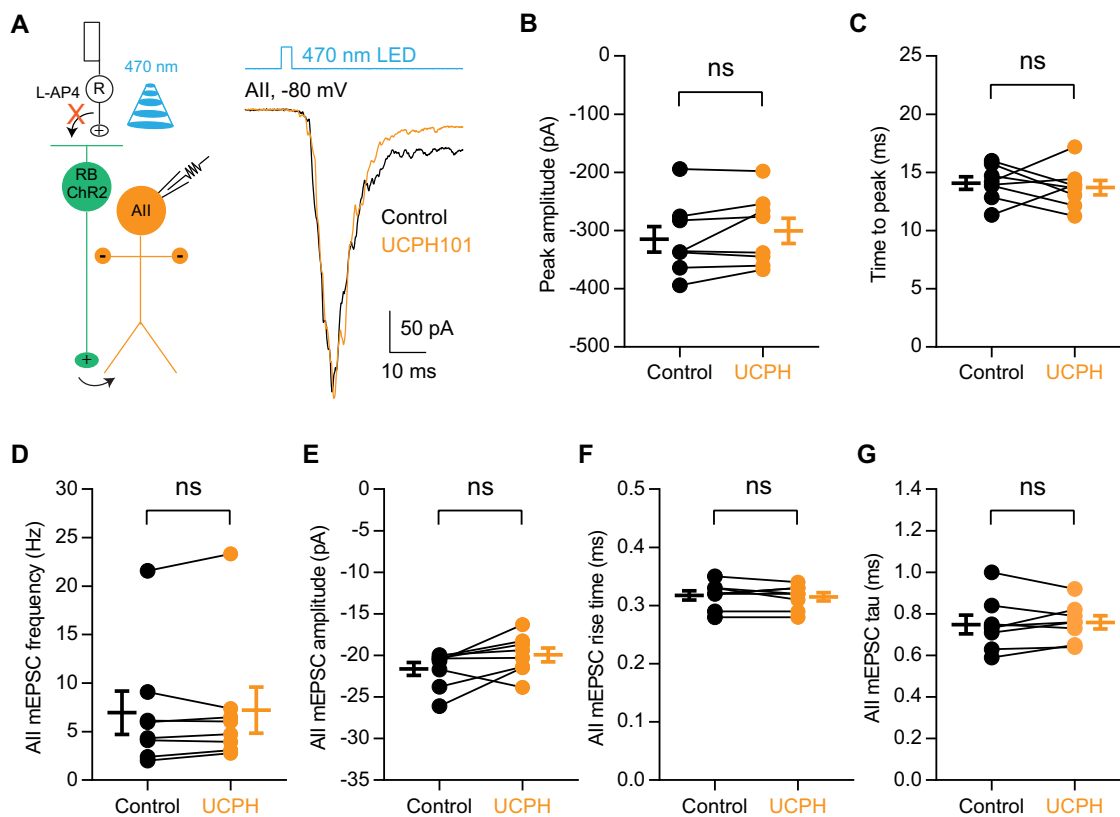


Figure 6. EAAT1 in Müller cells does not influence neurotransmission at RB→All synapses. **A**, The EPSCs recorded in All amacrine cells, which were evoked by activating Chr2+ RBs with 470-nm LED light stimulation, were not affected by 50 μ M UCPH101, a selective blocker of EAAT1 expressed exclusively in Müller cells. $V_{\text{hold}} = -80$ mV. R, rod; RB, rod bipolar cell; Chr2, channelrhodopsin-2. **B**, **C**, UCPH101 did not change the peak amplitude or time to peak of Chr2-evoked EPSCs ($n = 8$). **D–G**, UCPH101 did not influence the frequency, amplitude, rise time, or tau of mEPSCs recorded in Alls ($n = 8$). mEPSCs, miniature EPSCs. The data were represented as mean \pm SEM. Wilcoxon signed-rank test or Student's t test was used where appropriate. ns, not significantly different. See also Table 6.

mice under the same experimental condition ($n = 2$; data not shown).

Evoked EPSCs recorded in Alls were bidirectionally regulated by application of 200 μ M DHK, a selective EAAT2 blocker, and by application of 10 μ M GT949, a positive allosteric modulator of EAAT2 (Kortagere et al., 2018): DHK increased the peak amplitude of EPSCs ($118 \pm 4\%$ of control; $n = 7$), while GT949 reduced it ($78 \pm 3\%$ of control; $n = 10$; Fig. 4B–E; Table 4). We also examined the effect of 500 μ M DHK on All EPSCs, and found no significant differences in the relative effect on the peak amplitude between 200 and 500 μ M DHK (500 μ M DHK, $122 \pm 9\%$ of control, $n = 5$; 200 vs 500 μ M DHK, Welch's t test, $p = 0.7771$), indicating that EAAT2 is blocked completely by 200 μ M DHK under this experimental condition. Therefore, 200 μ M DHK was used in all subsequent experiments related to EAAT2. DHK also changed the kinetics of EPSCs (Table 4): the time to peak seemed to be reduced slightly, but not significantly (Fig. 4F), and accordingly, the rise time was decreased (Fig. 4G); however, the tau was not changed (Fig. 4H).

DHK, however, had no significant effects on the frequency, amplitude, rise time, or tau of mEPSCs recorded

in Alls (Fig. 4I–L; Table 4), indicating that blockade of EAAT2 does not influence spontaneous release from RB terminals and DHK has no effects on the biophysical properties of postsynaptic AMPA receptors on Alls.

It has been reported in the rat retina that in the presence of TBOA, a nonselective EAAT blocker, RBs are more depolarized in response to a positive current injection and the rise time of the EPSCs recorded in Alls is reduced when compared with the control condition; the effects of TBOA are thought to result from blocking EAAT5-mediated anion conductance in RB axon terminals (Veruki et al., 2006). To determine whether blockade of EAAT2 may influence the excitability of RBs, we tested the effect of DHK on membrane potential changes recorded in Chr2+ RBs which were evoked by brief flashes of light. Application of 200 μ M DHK increased the light-evoked voltage changes in RBs (Fig. 4M,N; Table 4), but did not affect the resting membrane potentials (Fig. 4O; Table 4).

Taken together, these results demonstrated that blockade of EAAT2 in RB axon terminals enhances and accelerates synaptic transmission at RB→All synapses, likely by increasing the light-evoked membrane potential changes in RBs.

Table 6: The effects of UCPH101 on All responses

	Data	Data structure	Type of test	Power	Mean \pm SEM	Number of cells
	Effect of UCPH on All EPSC amplitude					
	Control	Normal distribution			-315.00 ± 22.05	8
	50 μM UCPH	Normal distribution			-300.60 ± 21.52	8
a	Control vs UCPH		Paired Student's <i>t</i> test	$p = 0.1588$		8
	Effect of UCPH on All EPSC time to peak (unit: ms)					
	Control	Normal distribution			14.08 ± 0.53	8
	50 μM UCPH	Normal distribution			13.69 ± 0.63	8
b	Control vs UCPH		Paired Student's <i>t</i> test	$p = 0.6306$		8
	Effect of UCPH on All mEPSC frequency (unit: Hz)					
	Control	Normal distribution			6.95 ± 2.24	8
	50 μM UCPH	Normal distribution			7.22 ± 2.37	8
c	Control vs UCPH		Paired Student's <i>t</i> test	$p = 0.4685$		8
	DHK effect on All mEPSC amplitude (unit: pA)					
	Control	Normal distribution			-21.62 ± 0.78	8
	50 μM UCPH	Normal distribution			-19.94 ± 0.82	8
d	Control vs UCPH		Paired Student's <i>t</i> test	$p = 0.0707$		8
	Effect of UCPH on All mEPSC rise time (unit: ms)					
	Control	Non-normal distribution			0.32 ± 0.01	8
	50 μM UCPH	Normal distribution			0.32 ± 0.01	8
e	Control vs UCPH		Wilcoxon signed-rank test	$p = 0.8125$		8
	Effect of UCPH on All mEPSC tau (unit: ms)					
	Control	Normal distribution			0.75 ± 0.04	8
	50 μM UCPH	Normal distribution			0.76 ± 0.03	8
f	Control vs UCPH		Paired Student's <i>t</i> test	$p = 0.6382$		8

UCPH101, a selective EAAT1/GLAST blocker; All, All amacrine cell.

Pharmacological blockade of all EAATs has a significant effect on signal transmission at RB→All synapses

Since EAAT5 has also been reported to be present in the axon terminals of mouse RBs (Wersinger et al., 2006), one might want to know whether it may play a different role in regulating signal transmission at RB→All synapses. The fact that no selective blockers for EAAT5 are available, however, makes targeted pharmacological manipulation of EAAT5 impractical. Therefore, we compared the effects of DHK (blocking EAAT2 only) and TBOA (blocking all EAATs) on Chr2-evoked EPSCs in Alls to

determine whether other EAATs (e.g., EAAT5 in RBs and EAAT1 in Müller cells) may be involved in regulating neurotransmission at RB→All synapses.

Remarkably, Chr2-evoked EPSCs in Alls were enhanced substantially by application of 50 μM TBOA (Fig. 5A). Unlike DHK, which increased the transient component of EPSCs only (Fig. 4B), TBOA enhanced both the transient and sustained components (Fig. 5A,B; Table 5), with a much stronger effect on the latter (Fig. 5C; Table 5). When compared with DHK, TBOA had a greater effect on the transient component (Fig. 5D; Table 5). Furthermore, TBOA increased the time to peak, rise time and tau of

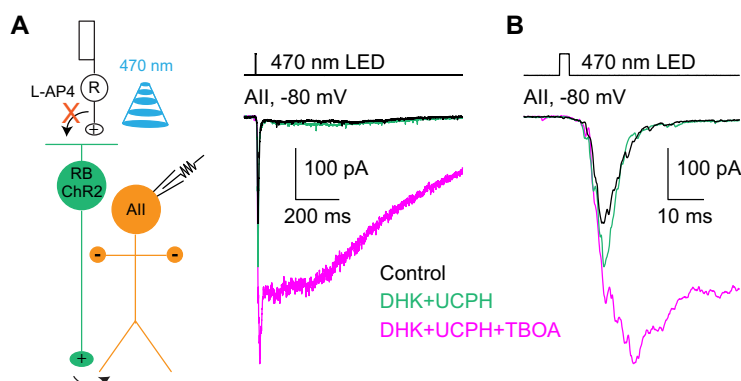


Figure 7. EAAT5 plays a predominant role in regulating neurotransmission at RB→All synapses. **A**, The EPSCs recorded in All amacrine cells, which were evoked by 470-nm LED light stimulation of ChR2-expressing RBs, were increased slightly by co-application of DHK (200 μM) and UCPH101 (50 μM ; $n = 8$), selective blockers of EAAT2 and EAAT1, respectively, and then enhanced more strongly by application of TBOA (50 μM ; $n = 3$), a nonselective blocker of all EAATs. $V_{\text{hold}} = -80$ mV. R, rod; RB, rod bipolar cell; ChR2, channelrhodopsin-2. **B**, Magnification of the traces shown in **A**.

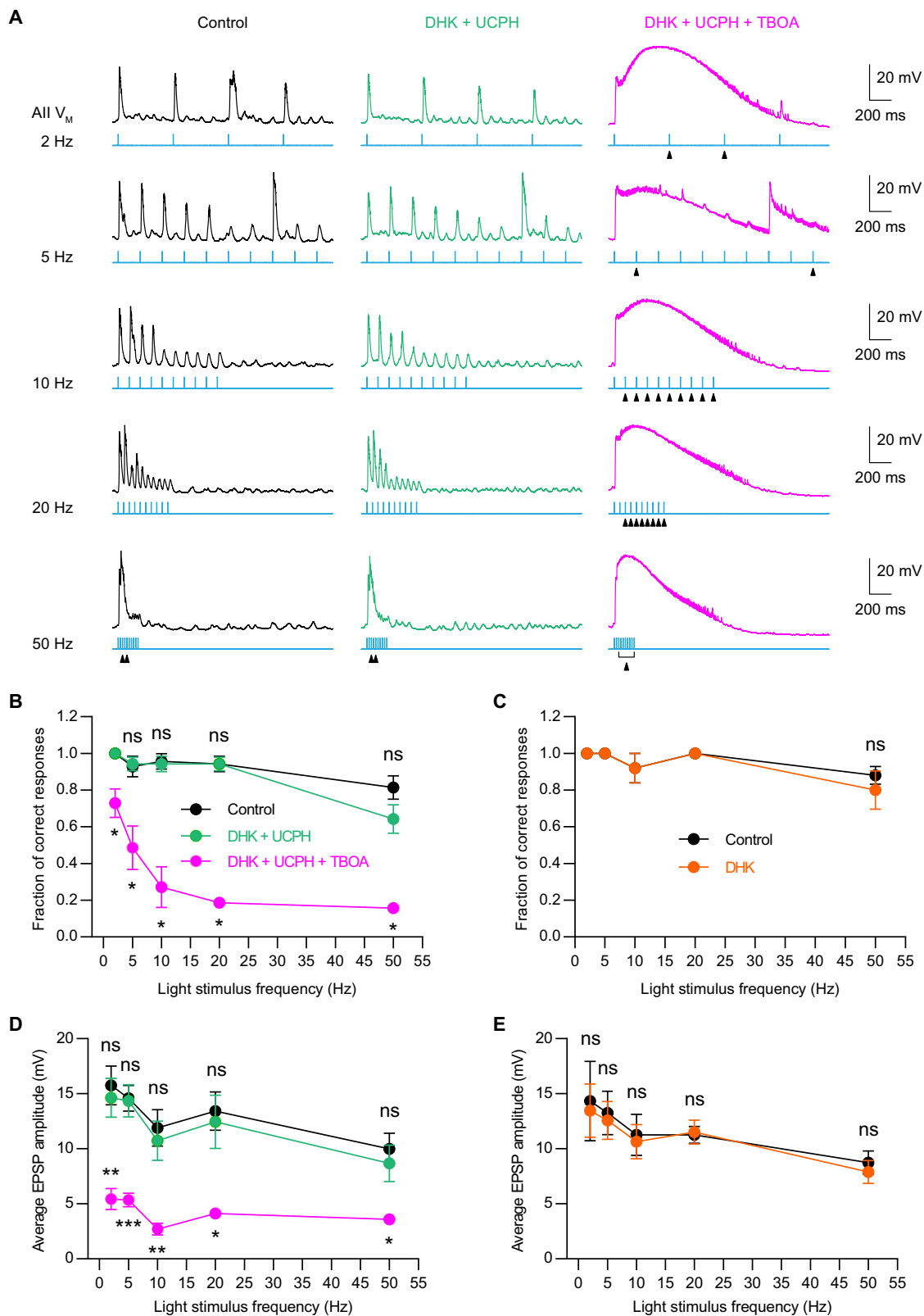


Figure 8. Blockade of presynaptic EAAT5 but not EAAT2 reduces temporal resolution at RB→All synapses. **A**, Representative traces showing the EPSPs recorded in All amacrine cells, which were evoked by activating ChR2-expressing RBs with 470-nm LED light stimulation. The frequencies of light stimulation were in the range of 2–50 Hz. Under the control condition, the membrane potentials of Alls could follow the 10 consecutive flashes very well even at stimulus frequency as high as 25 Hz (left panel). Co-application of 50 μM UCPH101, a selective EAAT1 blocker, and 200 μM DHK, a selective EAAT2 blocker, did not significantly influence Alls' responses to

continued

flashes (middle panel). But in the presence of 50 μM TBOA, a nonselective blocker of EAATs, AIs failed to respond to some individual flashes (marked by triangles; right panel), especially at stimulus frequencies higher than 10 Hz. **B**, Summary data showing the fractions of correct responses for AIs under three different experimental conditions. The fraction of correct responses was plotted as a function of light stimulus frequency. Application of 50 μM TBOA significantly reduced the fraction of correct responses at various stimulus frequencies ($n = 7$). **C**, Summary data showing the fractions of correct responses for AIs under control and DHK conditions. Application of 200 μM DHK did not significantly change the fraction of correct responses ($n = 5$). **D**, Summary data showing the average amplitudes of AI EPSPs under three different experimental conditions. The average EPSP amplitude was plotted as a function of light stimulus frequency. Application of 50 μM TBOA significantly reduced the average EPSP amplitude at various stimulus frequencies ($n = 7$). **E**, Summary data showing the average amplitudes of AI EPSPs under control and DHK conditions. Application of 200 μM DHK did not significantly change the average EPSP amplitude ($n = 5$). The data were represented as mean \pm SEM. Wilcoxon signed-rank test or paired t test was used for comparison. * $p < 0.05$, ** $p < 0.01$, *** $p < 0.001$; ns, not significantly different. See also Tables 7 and 8.

EPSCs (Fig. 5E–G; Table 5), suggesting that, in the presence of TBOA, a huge amount of glutamate accumulating in the synaptic cleft might diffuse to the postsynaptic sites and activate glutamate receptors asynchronously; and accordingly, glutamate might diffuse out of the synaptic cleft very slowly under this experimental condition. Apparently, pharmacological blockade of all EAATs had a much stronger effect on AI EPSCs than blocking EAAT2 only, indicating that EAATs other than EAAT2 also are involved in regulating synaptic transmission at RB→All synapses.

By contrast, TBOA did not influence the frequency, amplitude, or rise time of mEPSCs recorded in AIs (Fig. 5H–J; Table 5), indicating that blockade of all EAATs does not affect spontaneous release from RB terminals. Interestingly, TBOA seemed to increase the tau of mEPSCs slightly (Fig. 5K; Table 5). The relative effect of TBOA on the tau of mEPSCs ($107 \pm 3\%$ of control, $n = 7$), however, was much smaller than its effect on the tau of EPSCs ($911 \pm 317\%$ of control; $n = 7$), and thus could not account for the large effect of TBOA on synaptic transmission at RB→All synapses.

To determine to what extent blockade of both EAAT2 and EAAT5 may influence the excitability of RBs, we tested the effect of TBOA on membrane potential changes in ChR2+ RBs evoked by brief flashes of light. Similar to our observations with DHK (Fig. 4L,M), application of 50 μM TBOA increased the light-evoked voltage changes in RBs (Fig. 5L,M; Table 5), but did not affect the resting membrane potentials (Table 5). It is noteworthy that in the presence of TBOA, a large afterhyperpolarization (AHP) could be observed following the fast light-evoked depolarization of each recorded RB (Fig. 5L). The relative effects of DHK and TBOA on the fast depolarizations of RBs were not significantly different (Fig. 5N; Table 5), indicating that blockade of EAAT2 but not EAAT5 makes RBs more depolarized in response to light stimulation than the control condition; this is in contrast to the traditional view which attributes the effect of TBOA on RB membrane potentials to blocking EAAT5-mediated Cl⁻ conductance (Veruki et al., 2006).

EAAT1/GLAST in Müller cells does not influence neurotransmission at RB→All synapses

EAAT1 (also called GLAST), the glutamate transporter exclusively expressed in Müller glial cells, is thought to be responsible for the major retinal glutamate uptake (Derouiche and Rauen, 1995; Rauen et al., 1996; Harada et al., 1998;

Pow et al., 2000; Fyk-Kolodziej et al., 2004). Genetic deletion, antisense knock-down or pharmacological blockade of GLAST in mouse or rat retinas severely compromises the b-wave amplitudes of dark-adapted electroretinograms (ERGs), suggesting that GLAST in Müller cells might be involved in regulating the activities of RBs (Harada et al., 1998; Barnett and Pow, 2000; Tse et al., 2014). To determine whether GLAST may be involved in regulating neurotransmission at RB→All synapses, we recorded ChR2-evoked EPSCs in AIs and tested the effect of UCPH101, a selective GLAST blocker. Application of 50 μM UCPH101, however, did not have any significant effect on the peak amplitude or time to peak of EPSCs (Fig. 6A–C; Table 6).

In addition, UCPH101 did not affect the frequency, amplitude, rise time, or tau of mEPSCs recorded in AIs (Fig. 6D–G; Table 6), indicating that blockade of GLAST in Müller cells does not influence spontaneous release from RB terminals.

These results therefore demonstrated that glutamate uptake by Müller cells does not influence synaptic transmission from RB terminals.

EAAT5 plays a predominant role in regulating neurotransmission at RB→All synapses

The considerably stronger effect of TBOA than DHK and UCPH101 on ChR2-evoked EPSCs in AIs led us to the hypothesis that EAAT5 played a predominant role in regulating synaptic transmission at RB→All synapses. To test this hypothesis, we examined the effect of TBOA on ChR2-evoked EPSCs under the experimental condition in which EAAT2 and GLAST were blocked by DHK and UCPH101. In general, co-application of 200 μM DHK and 50 μM UCPH101 ($n = 8$) generated similar effect to that of DHK applied alone on AI EPSCs ($n = 7$); and in the presence of DHK and UCPH101, application of TBOA enhanced both the transient and sustained components of EPSCs significantly ($n = 3$; Fig. 7).

Taken together, these results proved our hypothesis that EAAT5 plays a predominant role in regulating synaptic transmission at RB→All synapses.

Blockade of presynaptic EAAT5 but not EAAT2 reduces temporal resolution at RB→All synapses

A recent study with EAAT5 knock-out mice has revealed an important role of EAAT5 for improving temporal resolution in the mouse retina, especially under mesopic

Table 7: The effects of EAAT-related drugs on the fraction of correct responses in Alls at various light stimulus frequencies

Data	Data structure	Type of test	Power	Mean \pm SEM	Number of cells
Effects of DHK, UCPH101 and TBOA on the fraction of correct responses in Alls at various stimulus frequencies					
2-Hz stimulus frequency					
Control	Non-normal distribution			1.00 \pm 0.00	7
200 μ M DHK + 50 μ M UCPH101	Non-normal distribution			1.00 \pm 0.00	7
200 μ M DHK + 50 μ M UCPH101 + 50 μ M TBOA	Normal distribution			0.73 \pm 0.08	7
a Control vs DHK + UCPH		Wilcoxon signed-rank test	N/A		7
b DHK + UCPH vs DHK + UCPH + TBOA		Wilcoxon signed-rank test	$p = 0.0313$		7
5-Hz stimulus frequency					
Control	Non-normal distribution			0.93 \pm 0.06	7
200 μ M DHK + 50 μ M UCPH101	Non-normal distribution			0.94 \pm 0.04	7
200 μ M DHK + 50 μ M UCPH101 + 50 μ M TBOA	Normal distribution			0.49 \pm 0.12	7
c Control vs DHK + UCPH		Wilcoxon signed-rank test	$p > 0.9999$		7
d DHK + UCPH vs DHK + UCPH + TBOA		Wilcoxon signed-rank test	$p = 0.0313$		7
10-Hz stimulus frequency					
Control	Non-normal distribution			0.96 \pm 0.04	7
200 μ M DHK + 50 μ M UCPH101	Non-normal distribution			0.94 \pm 0.04	7
200 μ M DHK + 50 μ M UCPH101 + 50 μ M TBOA	Non-normal distribution			0.27 \pm 0.11	7
e Control vs DHK + UCPH		Wilcoxon signed-rank test	$p > 0.9999$		7
f DHK + UCPH vs DHK + UCPH + TBOA		Wilcoxon signed-rank test	$p = 0.0156$		7
20-Hz stimulus frequency					
Control	Non-normal distribution			0.94 \pm 0.04	7
200 μ M DHK + 50 μ M UCPH101	Non-normal distribution			0.94 \pm 0.04	7
200 μ M DHK + 50 μ M UCPH101 + 50 μ M TBOA	Normal distribution			0.19 \pm 0.03	7
g Control vs DHK + UCPH		Wilcoxon signed-rank test	$p > 0.9999$		7
h DHK + UCPH vs DHK + UCPH + TBOA		Wilcoxon signed-rank test	$p = 0.0156$		7
50-Hz stimulus frequency					
Control	Normal distribution			0.81 \pm 0.06	7
200 μ M DHK + 50 μ M UCPH101	Normal distribution			0.64 \pm 0.08	7
200 μ M DHK + 50 μ M UCPH101 + 50 μ M TBOA	Non-normal distribution			0.16 \pm 0.03	7
i Control vs DHK + UCPH		Paired t test	$p = 0.0533$		7
j DHK + UCPH vs DHK + UCPH + TBOA		Wilcoxon signed-rank test	$p = 0.0156$		7
Effects of DHK alone on the fraction of correct responses in Alls at various stimulus frequencies					
2-Hz stimulus frequency					
Control	Non-normal distribution			1.00 \pm 0.00	5
200 μ M DHK	Non-normal distribution			1.00 \pm 0.00	5
k Control vs DHK		Wilcoxon signed-rank test	N/A		5
5-Hz stimulus frequency					
Control	Non-normal distribution			1.00 \pm 0.00	5
200 μ M DHK	Non-normal distribution			1.00 \pm 0.00	5
l Control vs DHK		Wilcoxon signed-rank test	N/A		5
10-Hz stimulus frequency					
Control	Non-normal distribution			0.92 \pm 0.08	5
200 μ M DHK	Non-normal distribution			0.92 \pm 0.08	5
m Control vs DHK		Wilcoxon signed-rank test	N/A		5
20-Hz stimulus frequency					

(Continued)

Table 7: Continued

Data	Data structure	Type of test	Power	Mean \pm SEM	Number of cells
Control	Non-normal distribution			1.00 \pm 0.00	5
200 μ M DHK	Non-normal distribution			1.00 \pm 0.00	5
n Control vs DHK		Wilcoxon signed-rank test	N/A		5
50-Hz stimulus frequency					
Control	Non-normal distribution			0.88 \pm 0.05	5
200 μ M DHK	Normal distribution			0.80 \pm 0.10	5
o Control vs DHK		Wilcoxon signed-rank test	$p = 0.5000$		5

TBOA, a non-selective EAAT blocker; UCPH101, a selective EAAT1/GLAST blocker; DHK, a selective EAAT2 blocker; All, All amacrine cell; N/A, not applicable.

light conditions (Gehlen et al., 2021). It is likely that genetic ablation of EAAT5 primarily affects signal transmission in the rod bipolar pathway (Gehlen et al., 2021), which functions under both scotopic and mesopic conditions (Ke et al., 2014). Because rods and RBs, both of which are essential neurons in the rod bipolar pathway, express EAAT5, the exact sites that may influence temporal resolution, however, remain to be determined.

We recorded EPSPs from Alls, which were evoked by activating Chr2-expressing RBs with a stimulus train of 10 consecutive flashes at various frequencies, and tested the effects of EAAT-related drugs. The frequencies of light stimulation were in the range of 2–50 Hz. Under the control condition, EPSPs recorded in Alls could follow the individual flashes very well even at the stimulus frequency as high as 25 Hz; at the stimulus frequency of 50 Hz, there was relatively high possibility that Alls only responded to some, but not all, flashes in a stimulus train (five of seven cells; Fig. 8A,B; Table 7). Blockade of EAAT1 and EAAT2 by co-application of 50 μ M UCPH101 and 200 μ M DHK did not make significant differences (Fig. 8A,B; Table 7). Under the experimental condition with subsequent application of 50 μ M TBOA to block EAAT5 in RBs, however, Alls failed to respond to some individual flashes, and at the stimulus frequencies of 10 Hz and higher, Alls were able to respond to the first one or two flashes only (Fig. 8A,B; Table 7). In contrast, blockade of EAAT2 by application of 200 μ M DHK alone did not influence Alls' responses to flashes at various frequencies (Fig. 8C; Table 7).

The All responses to individual flashes were also quantified by measuring the trough to peak EPSP amplitudes. Because the EPSP amplitudes varied greatly (Fig. 8A), we used the average amplitude of All EPSPs in response to a stimulus train of 10 flashes for comparisons between different experimental conditions. Under the control condition, the average EPSP amplitude seemed to decrease gradually as the light stimulus frequency increased, albeit with a sag at the stimulus frequency of 10 Hz (Fig. 8D,E). Application of DHK alone or co-application of UCPH101 and DHK did not change the average EPSP amplitude significantly, but subsequent application of TBOA strongly reduced it (Fig. 8D,E; Table 8).

In conclusion, these results demonstrated that EAAT5 but not EAAT2 in RBs plays an important role in improving temporal resolution at RB→All synapses.

Discussion

We combined molecular and functional analyses to determine the expression profiles, subcellular localization and functional roles of EAATs in mouse RBs. We found that EAAT2, together with the recently reported EAAT5 (Gehlen et al., 2021), are co-expressed in RB axon terminals near the release sites, thus revealing a common strategy (i.e., co-expression of EAAT2 and EAAT5) for the first (rod→RB synapse) and second (RB→All synapse) visual synapses that function under dim light conditions. Additionally, we demonstrated that EAAT2 and EAAT5 shape synaptic transmission from RB terminals in significantly different ways, likely via distinct mechanisms. Although expression of EAAT2 has been extensively studied in BCs of various species since 1990s, the present work, to the best of our knowledge, is the first report about the function of EAAT2 in the inner retina. Finally, we also found that EAAT5 but not EAAT2 plays a predominant role in regulating temporal resolution at RB→All synapses.

The function of EAAT2 in the retina

It has been well established that EAAT2 primarily serves as an astroglial glutamate transporter in the CNS (Tzingounis and Wadiche, 2007; Danbolt et al., 2016; Rodríguez-Campuzano and Ortega, 2021). In the mammalian retina, however, EAAT2 is mainly expressed in the neurons such as photoreceptors and BCs. Although the expression patterns of EAAT2, including its splice variants GLT-1 α , GLT-1B, and GLT-1v, have been studied extensively in the retinas of various species (Rauen and Kanner, 1994; Rauen et al., 1996, 2004; Eliasof et al., 1998b; Harada et al., 1998; Haverkamp and Wässle, 2000; Vandenbranden et al., 2000; Reye et al., 2002a, b; Fyk-Kolodziej et al., 2004; Niklaus et al., 2017), our current knowledge about the function of EAAT2 in retinal neurons is still limited. In lower vertebrates such as salamander, goldfish and zebrafish, EAAT2 in cone photoreceptors can modify the postsynaptic responses in horizontal cells or BCs (Gaal et al., 1998; Vandenbranden et al., 1996; Niklaus et al., 2017), whereas in mouse, EAAT2 does not influence neurotransmission at rod→RB synapse (Hasegawa et al., 2006). Also, genetic ablation or pharmacological blockade of EAAT2 in the mouse retina does not have any significant effect on the a-wave and b-wave amplitudes of dark-adapted ERGs, which reflect the activities of rod photoreceptors and RBs, respectively (Harada et al., 1998; Tse et al., 2014). However,

Table 8: The effects of EAAT-related drugs on the average amplitude of All EPSPs at various light stimulus frequencies

Data	Data structure	Type of test	Power	Mean \pm SEM	Number of cells
Effects of DHK, UCPH101 and TBOA on the average amplitude of All EPSPs at various stimulus frequencies					
2-Hz stimulus frequency					
Control	Normal distribution			15.75 \pm 1.77	7
200 μ M DHK + 50 μ M UCPH101	Normal distribution			14.62 \pm 1.77	7
200 μ M DHK + 50 μ M UCPH101 + 50 μ M TBOA	Normal distribution			5.44 \pm 0.97	7
a Control vs DHK + UCPH		Paired <i>t</i> test	<i>p</i> = 0.1704		7
b DHK + UCPH vs DHK + UCPH + TBOA		Paired <i>t</i> test	<i>p</i> = 0.0013		7
5-Hz stimulus frequency					
Control	Normal distribution			14.58 \pm 1.16	7
200 μ M DHK + 50 μ M UCPH101	Normal distribution			14.36 \pm 1.48	7
200 μ M DHK + 50 μ M UCPH101 + 50 μ M TBOA	Normal distribution			5.35 \pm 0.62	7
c Control vs DHK + UCPH		Paired <i>t</i> test	<i>p</i> = 0.7810		7
d DHK + UCPH vs DHK + UCPH + TBOA		Paired <i>t</i> test	<i>p</i> = 0.0007		7
10-Hz stimulus frequency					
Control	Normal distribution			11.90 \pm 1.66	7
200 μ M DHK + 50 μ M UCPH101	Normal distribution			10.74 \pm 1.79	7
200 μ M DHK + 50 μ M UCPH101 + 50 μ M TBOA	Normal distribution			2.70 \pm 0.52	7
e Control vs DHK + UCPH		Paired <i>t</i> test	<i>p</i> = 0.0746		7
f DHK + UCPH vs DHK + UCPH + TBOA		Paired <i>t</i> test	<i>p</i> = 0.0054		7
20-Hz stimulus frequency					
Control	Normal distribution			13.41 \pm 1.74	7
200 μ M DHK + 50 μ M UCPH101	Normal distribution			12.45 \pm 2.42	7
200 μ M DHK + 50 μ M UCPH101 + 50 μ M TBOA	Normal distribution			4.12 \pm 0.29	7
g Control vs DHK + UCPH		Paired <i>t</i> test	<i>p</i> = 0.4964		7
h DHK + UCPH vs DHK + UCPH + TBOA		Paired <i>t</i> test	<i>p</i> = 0.0116		7
50-Hz stimulus frequency					
Control	Normal distribution			9.99 \pm 1.42	7
200 μ M DHK + 50 μ M UCPH101	Normal distribution			8.67 \pm 1.65	7
200 μ M DHK + 50 μ M UCPH101 + 50 μ M TBOA	Non-normal distribution			3.58 \pm 0.24	7
i Control vs DHK + UCPH		Paired <i>t</i> test	<i>p</i> = 0.0763		7
j DHK + UCPH vs DHK + UCPH + TBOA		Wilcoxon signed-rank test	<i>p</i> = 0.0156		7
Effects of DHK alone on the average amplitude of All EPSPs at various stimulus frequencies					
2-Hz stimulus frequency					
Control	Normal distribution			14.33 \pm 3.61	5
200 μ M DHK	Normal distribution			13.46 \pm 2.41	5
k Control vs DHK		Paired <i>t</i> test	<i>p</i> = 0.6330		5
5-Hz stimulus frequency					
Control	Normal distribution			13.25 \pm 1.97	5
200 μ M DHK	Normal distribution			12.57 \pm 1.71	5
l Control vs DHK		Paired <i>t</i> test	<i>p</i> = 0.5547		5
10-Hz stimulus frequency					
Control	Normal distribution			11.26 \pm 1.87	5
200 μ M DHK	Normal distribution			10.65 \pm 1.55	5
m Control vs DHK		Paired <i>t</i> test	<i>p</i> = 0.4382		5
20-Hz stimulus frequency					

(Continued)

Table 8: Continued

Data	Data structure	Type of test	Power	Mean \pm SEM	Number of cells
Control	Normal distribution			11.26 \pm 0.76	5
200 μ M DHK	Normal distribution			11.51 \pm 1.08	5
n Control vs DHK		Paired <i>t</i> test	<i>p</i> = 0.8054		5
50-Hz stimulus frequency					
Control	Normal distribution			8.74 \pm 1.07	5
200 μ M DHK	Normal distribution			7.88 \pm 1.05	5
o Control vs DHK		Paired <i>t</i> test	<i>p</i> = 0.0780		5

TBOA, a non-selective EAAT blocker; UCPH101, a selective EAAT1/GLAST blocker; DHK, a selective EAAT2 blocker; All, All amacrine cell.

previous studies have shown the presence of EAAT2 in rod and cone photoreceptors of mouse, rat and human by immunohistochemistry (Rauen and Kanner, 1994; Haverkamp and Wässle, 2000; Rauen et al., 2004), and in this study our scRNA-seq analysis with mouse rod and cone transcriptomes detected EAAT2 mRNAs at reasonable levels (Fig. 1B). The functions of EAAT2 in mammalian rod and cone photoreceptors therefore remain to be further explored.

EAAT2 is found to be expressed in certain types of BCs in almost all the species studied. To date, however, no published studies have reported the function of EAAT2 in BCs. In the present work, we found that in the mouse retina, EAAT2 was expressed in all BC types while coexisting with EAAT5 in RBs and some cone BCs (Figs. 1, 2). Functionally, we showed that blockade of EAAT2 in RB axon terminals enhanced and accelerated the postsynaptic responses in Alls, likely by increasing the light-evoked voltage changes in RBs (Figs. 3, 4). Thus, in this study, we presented the first evidence that EAAT2 functions at BC ribbon synapses. Also, based on the distinct subcellular localizations of EAAT2 in different BC types (Fig. 3A; e.g., expression at the somata vs expression in the axon terminals), we could imagine that EAAT2 may play different roles in various BCs.

The function of EAAT5 in the retina

EAAT5 is originally known as a retina-specific glutamate transporter (Arriza et al., 1997), but recent studies also have reported that it is widely distributed in non-neuronal tissues (Lee et al., 2013). In the mouse and rat retinas, EAAT5 is mainly expressed in rod and cone photoreceptors as well as in BCs, including RBs (Pow and Barnett, 2000; Wersinger et al., 2006).

To date, functional studies about EAAT5 in the retina have been focused on the rod bipolar pathway which consists of both rod and RB, probably because of its strong immunolabeling at photoreceptor and RB axon terminals. At mouse rod \rightarrow RB synapses, EAAT5 plays a predominant role in regulating synaptic transmission: blockade of EAAT5 enhances and prolongs the postsynaptic responses of RBs (Hasegawa et al., 2006). Model simulations suggest that EAAT5 proteins densely packed near the release sites in rod terminals are essential for rapid removal of glutamate within the synaptic cleft (Hasegawa et al., 2006). At mouse and rat RB terminals, however, EAAT5 is generally thought to function as a large-conductance, glutamate-activated chloride channel; once

activated by glutamate released from RBs, EAAT5 may contribute feedback inhibition to RB terminals and thus control the RB output (Arriza et al., 1997; Veruki et al., 2006; Wersinger et al., 2006; Gameiro et al., 2011; Schneider et al., 2014; Fahlke et al., 2016; Bligard et al., 2020; Lukasiewicz et al., 2021; Kovermann et al., 2022). Paired recordings of synaptically connected mouse RBs and Alls have shown that pharmacological blockade of EAATs by TBOA influences the postsynaptic responses in Alls, presumably by inhibiting the EAAT5-mediated Cl conductance and enhancing the membrane depolarizations in RBs (Veruki et al., 2006).

It is noteworthy, however, that previous observations of EAAT5 function in RBs rely mainly on the assumption that EAAT5 was the only subtype of EAATs expressed in the axon terminals of RBs. It is, then, quite striking that in our present work we found that EAAT2 also was expressed in RB axon terminals near release sites (Figs. 1-3). Therefore, those data achieved by previous studies for “EAAT5” function in RB terminals have to be interpreted very carefully.

We also found that the light-evoked depolarizations of RBs enhanced by DHK and TBOA were not significantly different (Figs. 4, 5), indicating that blockade of Cl conductance mediated by EAAT2 but not EAAT5 enhances the voltage changes in mouse RBs. In contrast, the effect of TBOA on the voltage changes in rat RBs is supposed to be mediated by blockade of EAAT5 (Veruki et al., 2006), mainly because of the observation of EAAT5 expression in the axon terminals of RBs by immunohistochemistry (Pow and Barnett, 2000). Because EAAT5 is generally thought to have a higher Cl conductance than EAAT2 (Schneider et al., 2014; Fahlke et al., 2016; Lukasiewicz et al., 2021; Kovermann et al., 2022), it was quite surprising that blockade of both EAAT2 and EAAT5 by TBOA did not generate a larger change in RB membrane potentials than blockade of EAAT2 alone by DHK (Fig. 5M). Nevertheless, it is worth noting that TBOA induced a large AHP following the fast depolarization of each RB (Fig. 5L). Thus, there exists the possibility that the putative effect of blocking EAAT5-mediated Cl conductance by TBOA on RB voltage change is partially counteracted by the AHP. The origin of the AHP, however, is still unknown. In the presence of TBOA, excess glutamate might activate metabotropic glutamate receptors in RBs, which would in turn enhance the activities of G protein-activated K⁺ (GIRK) channels (Saugstad et al., 1996; Sharon et al., 1997; Knoflach and

Kemp, 1998) or small conductance Ca^{2+} -activated K^+ (SK) channels (Sourdret et al., 2003; García-Negredo et al., 2014), and thereby induce the AHPs. The effect of TBOA on membrane potentials of RBs apparently could not account for its large, prolonged effect on All responses (Fig. 5A,L), suggesting that blockade of EAAT5 regulates neurotransmission at RB→All synapses presumably by blocking its ability of glutamate transport and/or glutamate buffering (Tzingounis and Wadiche, 2007), but not by blocking EAAT5-mediated Cl conductance.

Recently, a new EAAT5 knock-out mouse model has been generated and used to study the functional role(s) of EAAT5, and consequently, EAAT5 is found to be important for improving temporal resolution in the retina, probably by affecting the rod bipolar pathway in the mesopic range (Gehlen et al., 2021). In the present study, we demonstrated that pharmacological blockade of EAAT5 but not EAAT2 influenced temporal resolution at mouse RB→All synapses (Fig. 8). However, since the rod bipolar pathway operates under both scotopic and mesopic illuminations (Ke et al., 2014), we cannot differentiate between the two light levels under our experimental conditions. Given the similar effects of TBOA (both enhance and prolong the postsynaptic responses) on neurotransmission at rod→RB synapses (Hasegawa et al., 2006) and at RB→All synapses (Fig. 5), we could imagine that pharmacological blockade of EAAT5 also would influence temporal resolution at rod→RB synapses.

Co-expression of EAAT2 and EAAT5 in retinal neurons

Accumulating evidence from immunohistochemical studies has shown that EAAT2 and EAAT5 are very likely to coexist in rod and cone photoreceptors. Whether EAAT2 and EAAT5 may be co-expressed in any certain type of BCs, however, is unknown. In the present work, we found that EAAT2 and EAAT5 coexisted in RBs as well as in types 3B, 4, 5B, and 5C BCs (Fig. 1). Co-expression of EAAT2 and EAAT5, therefore, seems to be a common strategy used by both first-order and second-order retinal neurons. It will, then, be interesting to explore in future studies why some BC types express both subtypes of EAATs while others express EAAT2 only.

In the present work, we also found that EAAT2 and EAAT5 differentially shape signal transmission at RB→All synapses, presumably via distinct mechanisms (Figs. 4, 5, 8). Generally, blocking EAAT5 likely has a stronger effect on retinal signal transmission, this may explain the observations from previous studies showing that genetic ablation or pharmacological blockade of EAAT2 does not significantly influence the a-wave or b-wave amplitudes of dark-adapted ERGs (Harada et al., 1998; Tse et al., 2014).

The function of EAAT1/GLAST in retinal Müller cells

GLAST, which is exclusively expressed in Müller cells, is thought to be the major glutamate sink in the retina, this traditional notion is largely drawn from the observations in autoradiographic uptake studies in which exogenously-applied radiolabeled glutamate is absorbed mainly by Müller cells (Derouiche and Rauen, 1995; Rauen et al.,

1996, 1998; Pow et al., 2000). In addition, genetic ablation, antisense knock-down or pharmacological blockade (i.e., by UCPH101) of GLAST in rodents severely reduces the b-wave amplitudes of dark-adapted ERGs, suggesting that GLAST in Müller cells might be involved in regulating the activities of RBs (Harada et al., 1998; Barnett and Pow, 2000; Tse et al., 2014).

However, there are also some electrophysiological studies arguing that glutamate uptake by Müller cells is not a fast and efficient process for regulating synaptic transmission (Gaal et al., 1998; Hasegawa et al., 2006; Rowan et al., 2010). The electrically evoked RB responses in GLAST knock-out mice were not different from those in wild-type mice, indicating that GLAST in Müller cells may not play a predominant role at rod→RB synapses (Hasegawa et al., 2006). Consistent with these results, in the present study, we provided direct evidence that blockade of GLAST in Müller cells does not influence neurotransmission at RB→All synapses (Fig. 6). Therefore, it would seem likely that GLAST in Müller cells plays a predominant role in removing glutamate diffused out of the synaptic cleft to prevent excitotoxicity, but a less important role in regulating synaptic transmission directly.

References

- Arriza JL, Eliasof S, Kavanaugh MP, Amara SG (1997) Excitatory amino acid transporter 5, a retinal glutamate transporter coupled to a chloride conductance. *Proc Natl Acad Sci USA* 94:4155–4160.
- Barnett NL, Pow DV (2000) Antisense knockdown of GLAST, a glial glutamate transporter, compromises retinal function. *Invest Ophthalmol Vis Sci* 41:585–591.
- Bligard GW, DeBrecht J, Smith RG, Lukasiewicz PD (2020) Light-evoked glutamate transporter EAAT5 activation coordinates with conventional feedback inhibition to control rod bipolar cell output. *J Neurophysiol* 123:1828–1837.
- Blondel VD, Guillaume JL, Lambiotte R, Lefebvre E (2008) Fast unfolding of communities in large networks. *J Stat Mech* 2008: P10008.
- Cho S, von Gersdorff H (2012) Ca^{2+} influx and neurotransmitter release at ribbon synapses. *Cell Calcium* 52:208–216.
- Danbolt NC, Furness DN, Zhou Y (2016) Neuronal vs glial glutamate uptake: resolving the conundrum. *Neurochem Int* 98:29–45.
- Derouiche A, Rauen T (1995) Coincidence of L-glutamate/L-aspartate transporter (GLAST) and glutamine synthetase (GS) immunoreactions in retinal glia: evidence for coupling of GLAST and GS in transmitter clearance. *J Neurosci Res* 42:131–143.
- Eliasof S, Arriza JL, Leighton BH, Amara SG, Kavanaugh MP (1998a) Localization and function of five glutamate transporters cloned from the salamander retina. *Vision Res* 38:1443–1454.
- Eliasof S, Arriza JL, Leighton BH, Kavanaugh MP, Amara SG (1998b) Excitatory amino acid transporters of the salamander retina: identification, localization, and function. *J Neurosci* 18:698–712.
- Euler T, Haverkamp S, Schubert T, Baden T (2014) Retinal bipolar cells: elementary building blocks of vision. *Nat Rev Neurosci* 15:507–519.
- Fahlke C, Körtzak D, Machtens JP (2016) Molecular physiology of EAAT anion channels. *Pflugers Arch* 468:491–502.
- Fairman WA, Vandenberg RJ, Arriza JL, Kavanaugh MP, Amara SG (1995) An excitatory amino-acid transporter with properties of a ligand-gated chloride channel. *Nature* 375:599–603.

- Fyk-Kolodziej B, Qin P, Dzhagaryan A, Pourcho RG (2004) Differential cellular and subcellular distribution of glutamate transporters in the cat retina. *Vis Neurosci* 21:551–565.
- Gaal L, Roska B, Picaud SA, Wu SM, Marc R, Werblin FS (1998) Postsynaptic response kinetics are controlled by a glutamate transporter at cone photoreceptors. *J Neurophysiol* 79:190–196.
- Gameiro A, Braams S, Rauen T, Grewer C (2011) The discovery of slowness: low-capacity transport and slow anion channel gating by the glutamate transporter EAAT5. *Biophys J* 100:2623–2632.
- García-Negredo G, Soto D, Llorente J, Morató X, Galenkamp KM, Gómez-Soler M, Fernández-Dueñas V, Watanabe M, Adelman JP, Shigemoto R, Fukazawa Y, Luján R, Ciruela F (2014) Coassembly and coupling of SK2 channels and mGlu5 receptors. *J Neurosci* 34:14793–14802.
- Gehlen J, Aretzweiler C, Mataruga A, Fahlke C, Müller F (2021) Excitatory amino acid transporter EAAT5 improves temporal resolution in the retina. *eNeuro* 8:ENEURO.0406-21.2021.
- Harada T, Harada C, Watanabe M, Inoue Y, Sakagawa T, Nakayama N, Sasaki S, Okuyama S, Watase K, Wada K, Tanaka K (1998) Functions of the two glutamate transporters GLAST and GLT-1 in the retina. *Proc Natl Acad Sci U S A* 95:4663–4666.
- Hasegawa J, Obara T, Tanaka K, Tachibana M (2006) High-density presynaptic transporters are required for glutamate removal from the first visual synapse. *Neuron* 50:63–74.
- Haverkamp S, Wässle H (2000) Immunocytochemical analysis of the mouse retina. *J Comp Neurol* 424:1–23.
- Ichinose T, Lukasiwicz PD (2012) The mode of retinal presynaptic inhibition switches with light intensity. *J Neurosci* 32:4360–4371.
- Ivanova E, Hwang GS, Pan ZH (2010) Characterization of transgenic mouse lines expressing Cre recombinase in the retina. *Neuroscience* 165:233–243.
- Kanai Y, Hediger MA (1992) Primary structure and functional characterization of a high-affinity glutamate transporter. *Nature* 360:467–471.
- Ke JB, Wang YV, Borghuis BG, Cembrowski MS, Riecke H, Kath WL, Demb JB, Singer JH (2014) Adaptation to background light enables contrast coding at rod bipolar cell synapses. *Neuron* 81:388–401.
- Knoflach F, Kemp JA (1998) Metabotropic glutamate group II receptors activate a G protein-coupled inwardly rectifying K⁺ current in neurones of the rat cerebellum. *J Physiol* 509:347–354.
- Kortagere S, Mortensen OV, Xia J, Lester W, Fang Y, Srikanth Y, Salvino JM, Fontana ACK (2018) Identification of novel allosteric modulators of glutamate transporter EAAT2. *ACS Chem Neurosci* 9:522–534.
- Kovermann P, Engels M, Müller F, Fahlke C (2022) Cellular physiology and pathophysiology of EAAT anion channels. *Front Cell Neurosci* 15:815279.
- Lagnado L, Schmitz F (2015) Ribbon synapses and visual processing in the retina. *Annu Rev Vis Sci* 1:235–262.
- Lee A, Anderson AR, Stevens M, Beasley S, Barnett NL, Pow DV (2013) Excitatory amino acid transporter 5 is widely expressed in peripheral tissues. *Eur J Histochem* 57:e11.
- Levine JH, Simonds EF, Bendall SC, Davis KL, Amir el AD, Tadmor MD, Litvin O, Fienberg HG, Jager A, Zunder ER, Finck R, Gedman AL, Radtke I, Downing JR, Pe'er D, Nolan GP (2015) Data-driven phenotypic dissection of AML reveals progenitor-like cells that correlate with prognosis. *Cell* 162:184–197.
- Liang CQ, Zhang G, Zhang L, Chen SY, Wang JN, Zhang TT, Singer JH, Ke JB (2021) Calmodulin bidirectionally regulates evoked and spontaneous neurotransmitter release at retinal ribbon synapses. *eNeuro* 8:ENEURO.0257-20.2020.
- Lukasiwicz PD, Bligard GW, DeBrecht JD (2021) EAAT5 glutamate transporter-mediated inhibition in the vertebrate retina. *Front Cell Neurosci* 15:62859.
- Machtens JP, Kortzak D, Lansche C, Leinenweber A, Kilian P, Begemann B, Zachariae U, Ewers D, de Groot BL, Briones R, Fahlke C (2015) Mechanisms of anion conduction by coupled glutamate transporters. *Cell* 160:542–553.
- Macosko EZ, Basu A, Satija R, Nemes J, Shekhar K, Goldman M, Tirosh I, Bialas AR, Kamitaki N, Martersteck EM, Trombetta JJ, Weitz DA, Sanes JR, Shalek AK, Regev A, McCarroll SA (2015) Highly parallel genome-wide expression profiling of individual cells using nanoliter droplets. *Cell* 161:1202–1214.
- Madisen L, et al. (2012) A toolbox of Cre-dependent optogenetic transgenic mice for light-induced activation and silencing. *Nat Neurosci* 15:793–802.
- Masland RH (2012) The neuronal organization of the retina. *Neuron* 76:266–280.
- Matthews G, Fuchs P (2010) The diverse roles of ribbon synapses in sensory neurotransmission. *Nat Rev Neurosci* 11:812–822.
- Niklaus S, Cadetti L, Vom Berg-Maurer CM, Lehnher A, Hotz AL, Forster IC, Gesemann M, Neuhaus SCF (2017) Shaping of signal transmission at the photoreceptor synapse by EAAT2 glutamate transporters. *eNeuro* 4:ENEURO.0339-16.2017.
- Pines G, Danbolt NC, Bjørås M, Zhang Y, Bendahan A, Eide L, Koepsell H, Storm-Mathisen J, Seeberg E, Kanner BI (1992) Cloning and expression of a rat brain L-glutamate transporter. *Nature* 360:464–467.
- Pow DV, Barnett NL (2000) Developmental expression of excitatory amino acid transporter 5: a photoreceptor and bipolar cell glutamate transporter in rat retina. *Neurosci Lett* 280:21–24.
- Pow DV, Barnett NL, Penfold P (2000) Are neuronal transporters relevant in retinal glutamate homeostasis? *Neurochem Int* 37:191–198.
- Rauen T, Kanner BI (1994) Localization of the glutamate transporter GLT-1 in rat and macaque monkey retinae. *Neurosci Lett* 169:137–140.
- Rauen T, Rothstein JD, Wässle H (1996) Differential expression of three glutamate transporter subtypes in the rat retina. *Cell Tissue Res* 286:325–336.
- Rauen T, Taylor WR, Kuhlbrodt K, Wiessner M (1998) High-affinity glutamate transporters in the rat retina: a major role of the glial glutamate transporter GLAST-1 in transmitter clearance. *Cell Tissue Res* 291:19–31.
- Rauen T, Wiessner M, Sullivan R, Lee A, Pow DV (2004) A new GLT1 splice variant: cloning and immunolocalization of GLT1c in the mammalian retina and brain. *Neurochem Int* 45:1095–1106.
- Reye P, Sullivan R, Fletcher EL, Pow DV (2002a) Distribution of two splice variants of the glutamate transporter GLT1 in the retinas of humans, monkeys, rabbits, rats, cats, and chickens. *J Comp Neurol* 445:1–12.
- Reye P, Sullivan R, Pow DV (2002b) Distribution of two splice variants of the glutamate transporter GLT-1 in the developing rat retina. *J Comp Neurol* 447:323–330.
- Rodríguez-Campuzano AG, Ortega A (2021) Glutamate transporters: critical components of glutamatergic transmission. *Neuropharmacology* 192:108602.
- Rowan MJ, Ripps H, Shen W (2010) Fast glutamate uptake via EAAT2 shapes the cone-mediated light offset response in bipolar cells. *J Physiol* 588:3943–3956.
- Saugstad JA, Segerson TP, Westbrook GL (1996) Metabotropic glutamate receptors activate G-protein-coupled inwardly rectifying potassium channels in *Xenopus* oocytes. *J Neurosci* 16:5979–5985.
- Schneider N, Cordeiro S, Machtens JP, Braams S, Rauen T, Fahlke C (2014) Functional properties of the retinal glutamate transporters GLT-1c and EAAT5. *J Biol Chem* 289:1815–1824.
- Seal RP, Amara SG (1999) Excitatory amino acid transporters: a family in flux. *Annu Rev Pharmacol Toxicol* 39:431–456.
- Sharon D, Vorobiov D, Dascal N (1997) Positive and negative coupling of the metabotropic glutamate receptors to a G protein-activated K⁺ channel, GIRK, in *Xenopus* oocytes. *J Gen Physiol* 109:477–490.
- Shekhar K, Lapan SW, Whitney IE, Tran NM, Macosko EZ, Kowalczyk M, Adiconis X, Levin JZ, Nemes J, Goldman M, McCarroll SA, Cepko CL, Regev A, Sanes JR (2016) Comprehensive classification of retinal bipolar neurons by single-cell transcriptomics. *Cell* 166:1308–1323.

- Sourdet V, Russier M, Daoudal G, Ankri N, Debanne D (2003) Long-term enhancement of neuronal excitability and temporal fidelity mediated by metabotropic glutamate receptor subtype 5. *J Neurosci* 23:10238–10248.
- Storck T, Schulte S, Hofmann K, Stoffel W (1992) Structure, expression, and functional analysis of a Na(+)-dependent glutamate/aspartate transporter from rat brain. *Proc Natl Acad Sci USA* 89:10955–10959.
- Tse DY, Chung I, Wu SM (2014) Pharmacological inhibitions of glutamate transporters EAAT1 and EAAT2 compromise glutamate transport in photoreceptor to ON-bipolar cell synapses. *Vision Res* 103:49–62.
- Tzingounis AV, Wadiche JI (2007) Glutamate transporters: confining runaway excitation by shaping synaptic transmission. *Nat Rev Neurosci* 8:935–947.
- Vandenberg RJ, Ryan RM (2013) Mechanisms of glutamate transport. *Physiol Rev* 93:1621–1657.
- Vandenbranden CA, Verweij J, Kamermans M, Müller LJ, Ruijter JM, Vrensen GF, Spekreijse H (1996) Clearance of neurotransmitter from the cone synaptic cleft in goldfish retina. *Vision Res* 36:3859–3874.
- Vandenbranden CA, Yazulla S, Studholme KM, Kamphuis W, Kamermans M (2000) Immunocytochemical localization of the glutamate transporter GLT-1 in goldfish (*Carassius auratus*) retina. *J Comp Neurol* 423:440–451.
- van der Maaten L, Hinton G (2008) Visualizing data using t-SNE. *J Mach Learn Res* 9:2579–2605.
- Veruki ML, Mørkve SH, Hartveit E (2006) Activation of a presynaptic glutamate transporter regulates synaptic transmission through electrical signaling. *Nat Neurosci* 9:1388–1396.
- Wersinger E, Schwab Y, Sahel JA, Rendon A, Pow DV, Picaud S, Roux MJ (2006) The glutamate transporter EAAT5 works as a presynaptic receptor in mouse rod bipolar cells. *J Physiol* 577:221–234.
- Zhang XM, Chen BY, Ng AH, Tanner JA, Tay D, So KF, Rachel RA, Copeland NG, Jenkins NA, Huang JD (2005) Transgenic mice expressing Cre-recombinase specifically in retinal rod bipolar neurons. *Invest Ophthalmol Vis Sci* 46:3515–3520.